City of Morro Bay and
Cayucos Sanitary District

OFFSHORE MONITORING AND REPORTING PROGRAM

FIRST QUARTER RECEIVING–WATER SURVEY

MARCH 2018

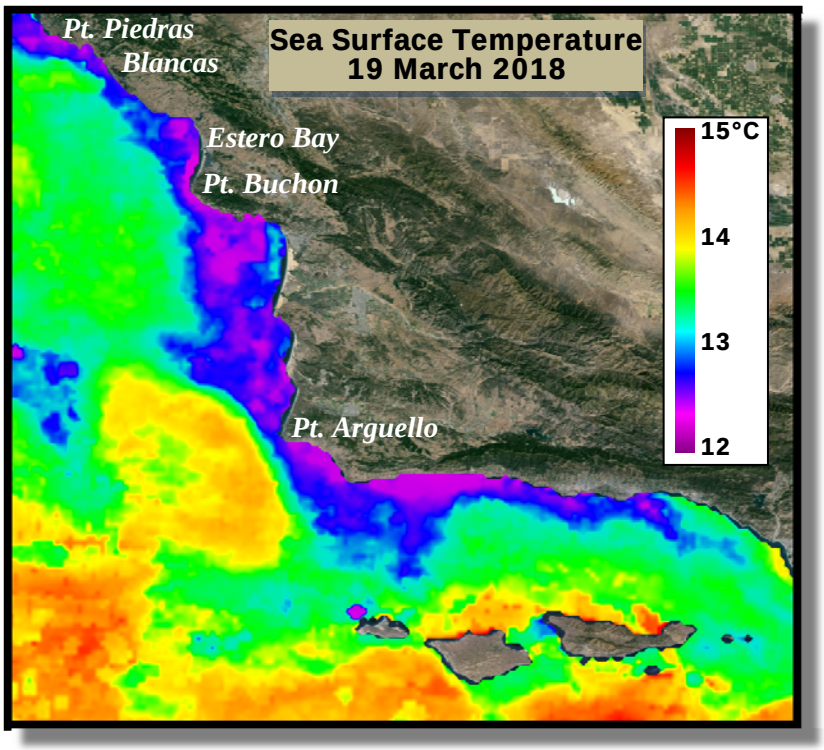

Marine Research Specialists
4744 Telephone Rd Ste 3 PMB 315
Ventura, California 93003

Report to the

City of Morro Bay and
Cayucos Sanitary District

955 Shasta Avenue
Morro Bay, California 93442
(805) 772-6272

OFFSHORE MONITORING AND REPORTING PROGRAM

FIRST QUARTER RECEIVING–WATER SURVEY

MARCH 2018

Prepared by

Douglas A. Coats

Marine Research Specialists

4744 Telephone Rd Ste 3 PMB 315
Ventura, California 93003

Telephone: (805) 644-1180
E-mail: Marine@Rain.org

April 2018

marine research specialists
4744 Telephone Rd., STE 3 PMB 315 • Ventura, CA 93003 • 805-644-1180

John Gunderlock
Wastewater & Collection Systems Supervisor
City of Morro Bay
955 Shasta Avenue
Morro Bay, CA 93442

26 April 2018

Reference: First Quarter Receiving-Water Survey Report – March 2018

Dear Mr. Gunderlock:

The attached report presents results from a quarterly receiving-water survey conducted on Monday, 12 March 2018. The survey was conducted in accordance with the requirements of the NPDES permit issued to the City and District for discharge of treated wastewater to Estero Bay. The report evaluated compliance with permit limitations and assessed the effectiveness of effluent dispersion within receiving waters. Quantitative analyses of continuous instrumental measurements and qualitative visual observations confirmed that the wastewater discharge complied with the receiving-water limitations specified in the permit, and with the objectives of the California Ocean Plan.

The offshore measurements confirmed that the diffuser structure and treatment plant continued to operate at a high level of performance. The measurements delineated a diffuse discharge plume containing low organic loads within a localized region surrounding the discharge point. Dilution within the plume exceeded expectations based on modeling and outfall design criteria.

This report constitutes the final receiving-water report for the MBCSD discharge. Receiving-water monitoring is no longer required under the provisions of the new discharge permit that became effective on 1 March 2018. This report augments 98 prior reports that documented the results of quarterly receiving-water surveys that were conducted by Marine Research Specialists over the past twenty-four years. Detailed quarterly and annual analyses of this comprehensive dataset have consistently demonstrated that the MBCSD discharge has not had a deleterious impact on seawater quality.

Contact the undersigned if you have questions regarding the attached report.

Sincerely,

Douglas A. Coats

Douglas A. Coats
Program Manager

I certify under penalty of law that this document and all attachments were prepared under my direction or supervision in accordance with a system designed to assure that qualified personnel properly gather and evaluate the information submitted. Based on my inquiry of the person or persons who manage the system, or those persons directly responsible for gathering the information, the information submitted is, to the best of my knowledge and belief, true, accurate and complete. I am aware that there are significant penalties for submitting false information, including the possibility of fine and imprisonment for knowing violations.

Mr. John Gunderlock
Wastewater/Collections System Supervisor
City of Morro Bay/Cayucos CSD Wastewater Treatment Plant

Date: 4/30/18

TABLE OF CONTENTS

LIST OF FIGURES

LIST OF TABLES

INTRODUCTION

The City of Morro Bay and the Cayucos Sanitary District (MBCSD) jointly own the wastewater treatment plant (WWTP) operated by the City of Morro Bay. In March 1985, Region IX of the U.S. Environmental Protection Agency (USEPA) and the Central Coast California Regional Water Quality Control Board (RWQCB) issued the first National Pollutant Discharge Elimination System (NPDES) permit to the MBCSD. The permit incorporated partially modified secondary treatment requirements for the plant's ocean discharge. The permit has been re-issued three times, in March 1993 (RWQCB-USEPA 1993ab), December 1998 (RWQCB-USEPA 1998ab), and January 2009 (RWQCB-USEPA 2009). The March 2018 field survey described in this report was the thirty-seventh receiving-water survey conducted under the most-recent permit issued in January 2009.

The January-2009 NPDES discharge permit requires seasonal monitoring of offshore receiving-water quality with quarterly surveys. This report summarizes the results of sampling conducted on 12 March 2018. Specifically, this first-quarter survey captured ambient oceanographic conditions along the central California coast during winter. The survey's measurements were used to assess the discharge's compliance with the objectives of the California Ocean Plan (COP) and the Central Coast Basin Plan (RWQCB 1994) as promulgated by the receiving-water limitations specified in the NPDES discharge permit.

The monitoring objectives were achieved by empirically evaluating tabulations of instrumental measurements and standard field observations. In addition to the traditional, vertical water-column profiles, instrumental measurements were used to generate horizontal maps from high-resolution data gathered by towing a CTD[1] instrument package repeatedly over the diffuser structure. This allowed for a more precise delineation of the plume's lateral extent.

SURVEY SETTING

The MBCSD treatment plant is located within the City of Morro Bay, which is situated along the central coast of California halfway between Los Angeles and San Francisco. Effluent is carried from the onshore treatment plant through a 1,450-m long outfall pipe, which terminates at a diffuser structure on the seafloor 827 m from the shoreline within Estero Bay (Figure 1). The diffuser structure extends an additional 52 m toward the northwest from the outfall terminus and consists of 34 ports that are hydraulically designed to create a turbulent ejection jet that rapidly mixes effluent with receiving seawater upon discharge. Currently, six of the diffuser ports are closed, thereby improving effluent dispersion by increasing the ejection velocity from the remaining 28 ports distributed along a 42-m section of the diffuser structure.

Following discharge from the diffuser ports, additional turbulent mixing occurs as the buoyant plume of dilute effluent ascends through the water column. Most of this buoyancy-induced mixing occurs within a zone of initial dilution (ZID), whose lateral reach in modeling studies extends 15.2 m from the centerline of the diffuser structure. Beyond the ZID, energetic waves, tides, and coastal currents within Estero Bay further disperse the dilute effluent within the open-ocean receiving waters. Both vertical hydrocasts and horizontal tow surveys are conducted around the diffuser structure to assess the efficacy of the diffuser, to define the lateral extent of the discharge plume, and to evaluate compliance with the NPDES permit limitations.

[1] Conductivity, temperature, and depth (CTD)

Figure 1. Location of the Receiving-Water Survey Area

Near the diffuser, prevailing flow generally follows bathymetric contours that parallel the north-south trend of the adjacent coastline. Because of the rapid initial mixing achieved within 15 m of the diffuser structure, impingement of unmixed effluent onto the adjacent coastline, 827 m away, is highly unlikely. Nevertheless, in the event of a failure in the treatment plant's disinfection system, collection and analysis of water samples at the eight surfzone-sampling stations shown in Figure 1 would be conducted to monitor for potential shoreline impacts. These surfzone samples would be analyzed for total and fecal coliform, and enterococcus bacterial densities.

Areas of special concern, such as the Morro Bay National Estuary and the Monterey Bay National Marine Sanctuary, are not affected by the discharge because they are even more distant from the outfall location. For example, the southern boundary of the Monterey Bay National Marine Sanctuary is located 38 km to the north, while the entrance to the Morro Bay National Estuary lies 2.8 km south. The southerly orientation of the mouth of the Bay, and the presence of Morro Rock 2 km to the south, serve to further limit direct seawater exchange between the discharge point and the Bay (Figure 1).

SAMPLING LOCATIONS

As shown in Figure 2, the offshore sampling pattern consists of six fixed offshore stations located within 100 m of the outfall diffuser structure. The red ⊙ symbols in the Figure indicate the target locations of the sampling stations (Table 1). The stations are situated at three distances relative to the center of the diffuser structure, and lie along a north-south axis at the same water depth (15.2 m) as the center of the diffuser. Depending on the direction of the local oceanic currents at the time of sampling, the discharge may influence seawater properties at one or more of these stations. The up-current stations on the opposite side of the diffuser then act as reference stations. Comparisons between the water properties at these antipodal stations quantify departures from ambient seawater properties caused by the discharge and allow compliance with the requirements of the NPDES discharge permit to be determined.

The finite size of the diffuser is an important consideration in the assessment of wastewater dispersion close to the discharge. Although the discharge is considered a "*point source*" for modeling and regulatory purposes, it does not occur at a single isolated point of infinitesimal size. Instead, the discharge is distributed along a 42 m section of the seafloor, and, ultimately, the amount of wastewater dispersion at a given point in the water column is dictated by its distance from the closest diffuser port, rather than its distance from the center of the diffuser structure. This "*closest approach*" distance can be considerably less than the centerpoint distance normally cited in modeling studies (compare the last two columns of Table 1).

Another important consideration for compliance evaluation is the ability to determine the actual location of the measurements. Discerning small spatial separations within the compact sampling pattern only became feasible after the advent of Differential Global Positioning Systems (DGPS). The accuracy of traditional navigation systems such as LORAN or standard GPS is typically ±15 m, a span equal to half the total width of the ZID itself. DGPS incorporates a second signal from a fixed, land-based beacon that continuously transmits position errors embedded within standard GPS readings to the DGPS receiver aboard the survey vessel. Real-time correction for these position errors provides an extremely stable and accurate offshore navigational reading with position errors of no more than 2 m, and often of sub-meter accuracy.

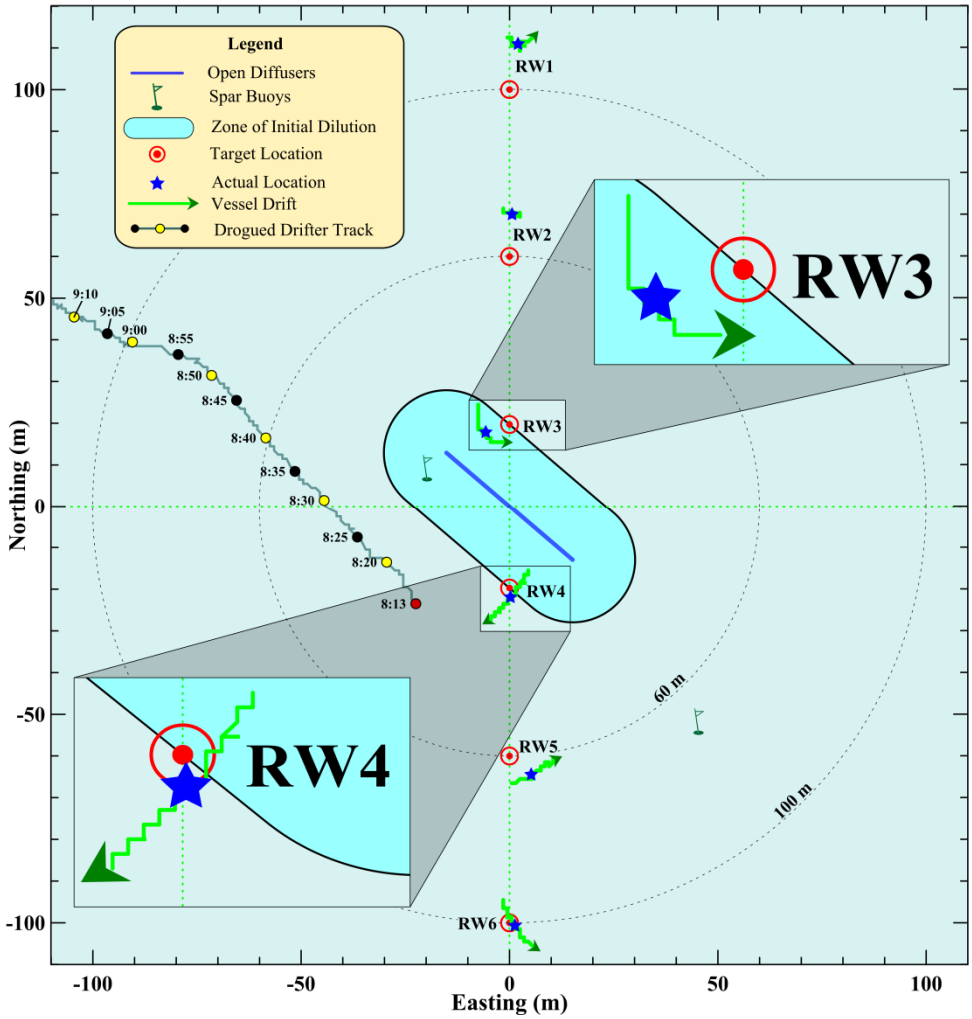

Figure 2. Station Locations

Table 1. Target Locations of the Receiving-Water Monitoring Stations

Station	Description	Latitude	Longitude	Center Distance[2] (m)	Closest Approach Distance[3] (m)
RW1	Upcoast Midfield	35° 23.253' N	120° 52.504' W	100	88.4
RW2	Upcoast Nearfield	35° 23.231' N	120° 52.504' W	60	49.4
RW3	Upcoast ZID	35° 23.210' N	120° 52.504' W	20	15.0
RW4	Downcoast ZID	35° 23.188' N	120° 52.504' W	20	15.0
RW5	Downcoast Nearfield	35° 23.167' N	120° 52.504' W	60	49.4
RW6	Downcoast Midfield	35° 23.145' N	120° 52.504' W	100	88.4

[2] Distance to the center of the open diffuser section
[3] Distance to the closest open diffuser port

During a diver survey in July 1998, the survey vessel's new DGPS navigation system, consisting of a Furuno™ GPS 30 and FBX2 differential beacon receiver, was used to precisely determine the position of the open section of the diffuser structure (MRS 1998) and establish the target locations for the receiving-water monitoring stations shown in Figure 2 and listed in Table 1. Presently, the use of two independent DGPS receivers aboard the survey vessel allows access to two separate land-based beacons for navigational intercomparison, ensuring extremely accurate and uninterrupted navigational reports.

Recording of DGPS positions at one-second intervals allows precise determination of sampling locations throughout the vertical CTD profiling conducted at the six individual stations, as well as during the tow survey. Knowledge of the precise location of individual CTD measurements relative to the diffuser is critical for accurate interpretation of the water-property fields. During vertical-profile sampling, for example, the actual measurement locations rarely coincide with the target coordinates listed in Table 1 because winds, waves, and currents induce unavoidable horizontal offsets (drift). Even during quiescent metocean[4] conditions, the residual momentum of the survey vessel as it approaches the target locations can create perceptible offsets. Using DGPS however, these offsets can be quantified, and the vessel location can be precisely tracked throughout sampling at each station.

The March 2018 hydrocasts were conducted progressing from north to south, beginning with Station RW1. The magnitude of the drift at each of the six stations during the March 2018 survey is apparent from the length of the green tracklines in Figure 2. The tracklines trace the horizontal movement of the CTD as it was lowered to the seafloor at each station. Their lengths and offsets from the target locations reflect the overall station-keeping ability during the March 2018 survey.

The time it took the CTD to traverse the water column to the seafloor, which averaged 1 min 13 s, was consistent among stations, while the lateral distance traversed by the instrument package varied considerably among the stations, ranging from less than 6 m at the northernmost Stations RW1 and RW2, to more than 10 m at the other Stations (Figure 2). Similarly, the direction of the drift was inconsistent among the stations. This variability arises because the lateral movement of the CTD at any given time is determined by the complex interplay between the external influences of winds and currents, and the vessel's residual momentum immediately prior to each downcast.

However, because relatively quiescent metocean conditions prevailed during the survey, drift was primarily determined by vessel residual momentum. For example, the southwestward drift at Station RW4 arose from the vessel's residual momentum as it approached the station from the northeast. Conversely, the northeastward drift direction at Station RW5 arose because of the vessel's approach from the southwest. In contrast, more aggressive use of reverse thrust as the vessel approached Station RW2 resulted in almost imperceptible movement of the CTD during the downcast there. Metocean's secondary influence on the movement of the vessel is apparent in the curvature of the trajectories at Stations RW1 and RW3.

Regardless of the cause, detailed knowledge of the CTD's movement during downcasts is important for the interpretation of the water-quality measurements. Because the target locations for Stations RW3 and RW4 lie along the ZID boundary (viz., the red ⊙ symbols in the insets of Figure 2), knowledge of the CTD's location during the downcasts at those stations is especially important in the compliance evaluation. This is because the receiving-water limitations specified in the COP only apply to

[4] Meteorological and oceanographic conditions include winds, waves, tides, and currents.

measurements recorded along or beyond the ZID boundary, where initial mixing is assumed complete. For example, during the March 2018 survey, data collected within the upper 6.5 m of the water column at Station RW4 were not subject to a compliance assessment because the CTD was located within the ZID during the initial portion of that downcast (refer to the lower left inset in Figure 2). The CTD traversed the ZID boundary as it was lowered through the water column and was transported toward the southwest. As a result, only data collected in the lower half of the water column were applicable to a compliance evaluation.[5] By comparison, all of the data collected at Station RW3 were excluded from the water-quality evaluation even though the downcast began when the CTD was only 1.25 m inside of the ZID boundary (upper right inset in Figure 2).

Compliance assessments notwithstanding, measurements acquired within the ZID lend valuable insight into the outfall's effectiveness at dispersing wastewater. For example, low dilution rates and concentrated effluent throughout the ZID would indicate potentially damaged or broken diffuser ports. Analysis of the outfall's operation over the past two and a half decades, however, demonstrates that it has consistently maintained a high level of effectiveness in effluent dispersal. In fact, without the occasional measurements recorded within the ZID due to vessel drift, the extremely dilute discharge plume might remain undetected within all the vertical profiles collected during a given survey.

It has not always been possible to determine which measurements were subject to permit limits among hydrocasts near the ZID boundary, however. For example, prior to 1999 and before the advent of DGPS, CTD locations could not be determined with sufficient accuracy to establish whether the average ZID station position was located within the ZID, much less, how the CTD was moving laterally during the hydrocast. Because of these navigational limitations, sampling was presumed to occur at a single, imprecisely determined, horizontal location. Federal and state reporting of monitoring data still mandates identification of a single position for all of the CTD data collected at a particular station. Thus, for regulatory reporting, and for consistency with past surveys, this survey report also identifies a single sampling location for each station. These average station positions are shown by the blue stars in Figure 2, and are listed in Table 2 along with their distances from the diffuser structure.

Table 2. Average Position of Vertical Profiles during the March 2018 Survey

Station	Time (PDT)		Latitude	Longitude	Closest Approach	
	Downcast	Upcast			Range[6](m)	Bearing[7](°T)
RW1	9:47:42	9:49:06	35° 23.259' N	120° 52.503' W	99.7	10
RW2	9:51:39	9:52:54	35° 23.237' N	120° 52.504' W	59.4	15
RW3	9:55:46	9:56:55	35° 23.209' N	120° 52.508' W	**10.0** [8]	41
RW4	9:59:02	10:00:13	35° 23.187' N	120° 52.504' W	**16.4** [9]	221
RW5	10:02:23	10:03:30	35° 23.164' N	120° 52.501' W	52.3	191
RW6	10:06:02	10:07:16	35° 23.145' N	120° 52.503' W	88.7	189

[5] The centers of the green arrowheads in Figure 2 mark the locations of the deepest measurements, which are collected immediately above the seafloor at each station.
[6] Distance from the closest open diffuser port to the average profile location
[7] Angle measured clockwise relative to true north from the closest diffuser port to the average profile location
[8] All of the CTD measurements were located within the ZID boundary (refer to upper right inset in Figure 2).
[9] Some of the CTD measurements were located within the ZID boundary (refer to lower left inset in Figure 2).

OCEANOGRAPHIC PROCESSES

The trajectory of a satellite-tracked drogued drifter measured oceanic flow throughout the March 2018 survey (Figure 3). Modeled after the curtain-shade design of Davis et al. (1982) and drogued at mid-depth (7 m), a drifter has been deployed during each of the quarterly water column surveys conducted over the past two decades. In this configuration, oceanic flow rather than surface wind dictates the drifter's trajectory, which provides a good indication of the plume's movement after discharge, except when the flow field exhibits strong vertical shear.

During the March 2018 survey, the drifter was deployed near the diffuser structure at 8:13 AM, and was recovered at 10:21 AM at a location 297 m northwest (315°T[10]) of its original release point (red dots in Figure 3). The nearly linear drifter track demonstrated that mid-depth oceanic current direction was comparatively consistent throughout the survey. However, current speeds increased perceptibly after 9:15 AM and immediately following a slight westward jog in the drifter trajectory that began around 8:50 AM.

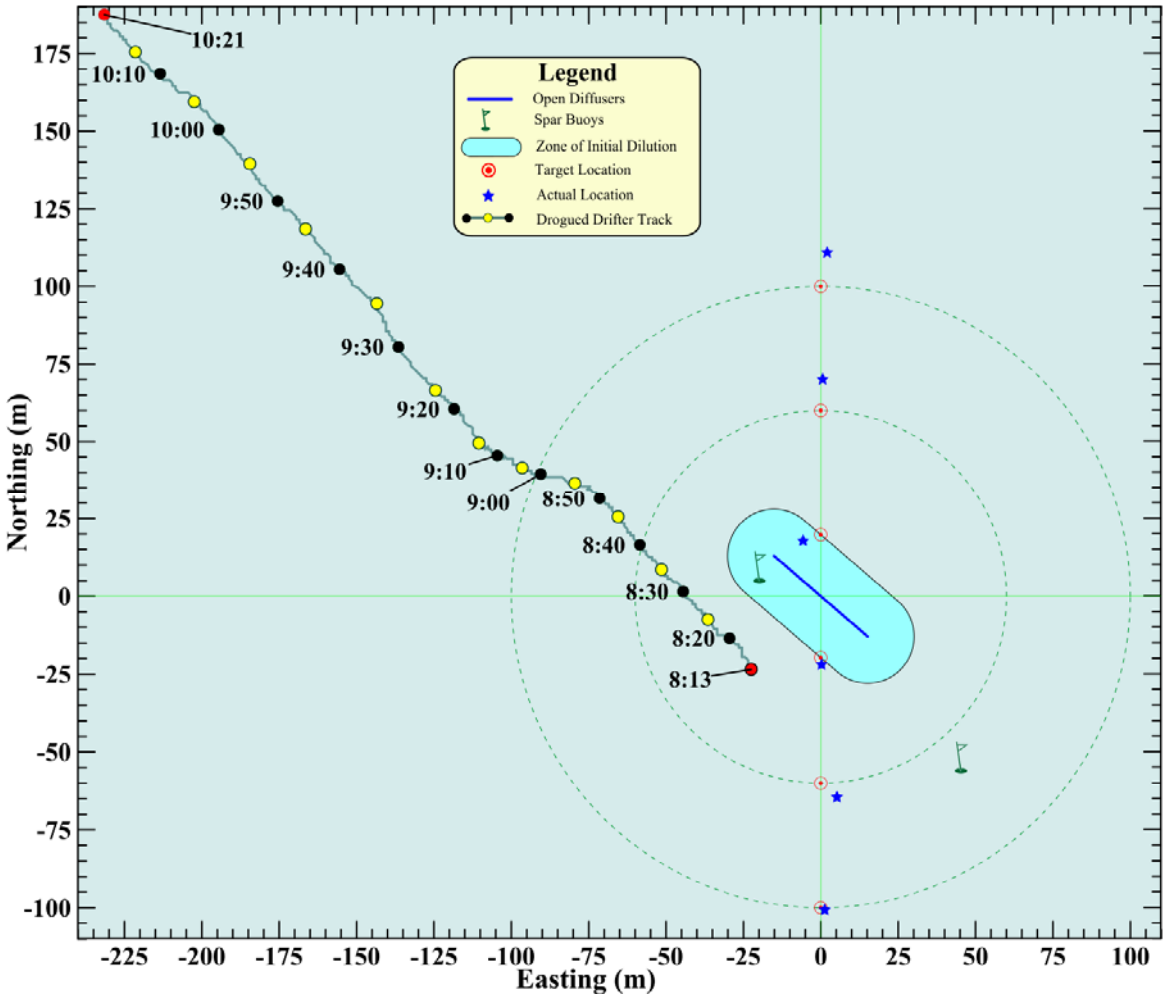

Figure 3. Drogued Drifter Trajectory

[10] Direction measured clockwise relative to true (rather than magnetic) north

The mid-survey change in oceanic flow speed is documented by the spacing between the yellow and black dots in Figure 3, which show the drifter's progress at five- and ten-minute intervals. The uniform spacing before and after this minor flow event indicates that flow speed varied little from the average speed of 3.3 cm/s[11] prior to the event, but increased to 4.5 cm/s during the last hour of the survey. The overall flow speed, however, was comparable to that of most other surveys, and indicated that effluent would have experienced only a brief, 6.6-minute residence time within the ZID at the time of the March 2018 survey.

The flow-speed change appears to coincide with increasing tidal flow speeds that could have occurred in conjunction with the outgoing tide that followed flow stagnation at the 8:00 AM peak flood tide (Figure 4). However, the overall drifter movement toward the northwest (Figure 3) was not consistent with the expected direction of ebb tidal flow that prevailed throughout most of the survey (yellow shading in Figure 4). When other physical oceanographic influences are negligible, an ebb tide tends to induce a weak southwestward (offshore) flow in the survey region.

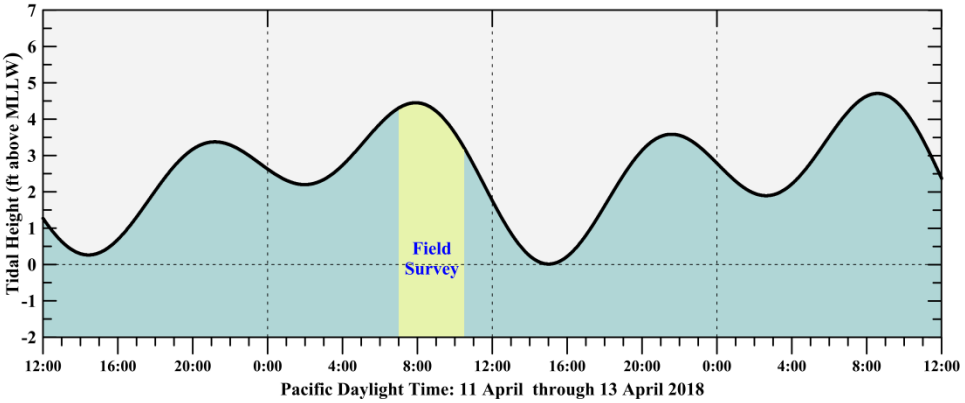

Figure 4. Tidal Level during the March 2018 Survey

Normally, however, oceanic flow within the survey area is influenced by a variety of other oceanographic processes, such as upwelling or remote forces that arise from large-scale along-shore pressure gradients and from the passing of large eddies embedded within the California Current. During most of the year, currents along this section of coastline are dominated by the prevailing wind field. Strong and steady northwesterly winds cause upwelling within the water column and produce a system of vertical countercurrents (Figure 5). Net flow within the upper water column, known as Ekman transport, occurs at a 90º angle to the right of the prevailing wind direction.[12] As a result, warm ocean waters within the surface mixed layer are driven offshore (southwestward) in response to the along-shore winds (toward the southeast). Near the coast, these warm surface waters are replaced by deep, cool, nutrient-rich waters that well up from below. The upwelled waters originate farther offshore and move shoreward (northeastward) along the seafloor to replace surface waters driven offshore by Ekman transport. Thus, strong upwelling establishes a vertically sheared cross-shore countercurrent within the survey area.

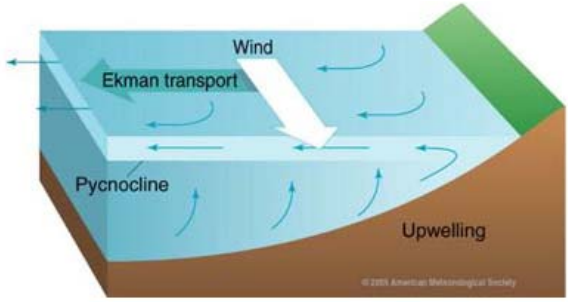

Figure 5. Schematic of Upwelling Processes

[11] 0.065 kt
[12] http://oceanmotion.org/html/background/upwelling-and-downwelling.htm

The onset of these upwelling-dominated processes normally begins with a rapid intensification of southeastward-directed winds along the central coast during late March and or early April as shown by the positive (blue) upwelling indices in Figure 6. This transition to more persistent southeastward winds is initiated by the stabilization of a high-pressure field over the northeastern Pacific Ocean. Clockwise winds around this pressure field drive prevailing northwesterly winds (i.e., toward the southeast) along the central California coast. Some degree of upwelling is almost always present during offshore surveys (yellow diamonds in Figure 6). Throughout most of the year, the nutrient-rich seawater brought to the sea surface near the coast by upwelling enables phytoplanktonic blooms that are the foundation of the productive marine fishery found along the central California coast. The vertical counterflow associated with persistent upwelling conditions also enhances vertical stratification of the water column. The influx of cold dense water at depth produces a thermocline that is commonly maintained throughout summer and into early fall.

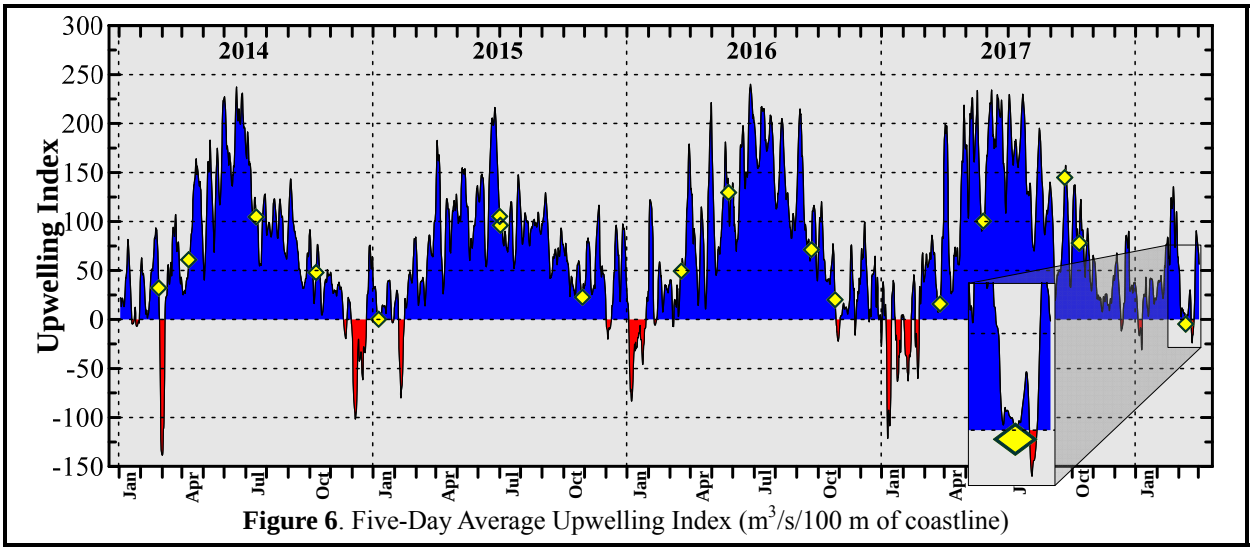

Figure 6. Five-Day Average Upwelling Index ($m^3/s/100$ m of coastline)

During late fall and winter, upwelling is typically weak, and occasionally downwelling events, indicated by the negative (red shaded) indices in Figure 6, occur when passing storms temporarily reverse the normal wind pattern and drive surface waters shoreward. As the surface waters approach the coastline, they downwell, producing nearly uniform seawater properties throughout the water column. An unusual series of severe winter storms at the beginning of 2017 produced multiple downwelling events (refer to the red downward excursions in the upwelling index during January and February 2017 in Figure 6).

Although winds were negligible at the time of the March 2018 survey, winds in the weeks prior to the survey were strong enough to produce a pattern of sea surface temperatures indicative of substantial upwelling along central coast (refer to the inset in Figure 6). Remnants of this pattern were captured by the satellite image shown on the cover of this report. The image was recorded by infrared sensors on one of NOAA's polar orbiting satellites during a period of relatively cloudless skies in the week following the survey. The presence of a band of cooler, upwelled water is visually apparent along the south-central coastline (dark -blue and magenta shading). However, the 2°C contrast between these sea-surface temperatures and temperatures farther offshore (in green and yellow) confirms that upwelling was weak at the time of the March 2018 survey. Nevertheless, the visually striking band of lower temperatures along the coastline demonstrates that even moderate upwelling can have a profound effect on oceanographic conditions throughout the region.

The inset in Figure 6 shows that the March 2018 survey was conducted shortly after a substantial early upwelling event that had an index exceeding 125 $m^3/s/100$ m of coastline. Nevertheless, as described below, the water column was only moderately stratified at the time of the March 2018 survey. The sharply defined thermocline normally indicative of an active upwelling event had largely been eroded by mixing; leaving behind a gradual vertical gradient in seawater properties after upwelling winds had relaxed. Thus, the northwestward oceanic flow measured within northern Estero Bay during the survey was probably not solely due to either tidal or upwelling forces. Instead, it is likely that it was largely driven by other external oceanographic processes, such as large-scale along-shore pressure gradients, or the passing of an eddy embedded within the California Current. In contrast to factors that influenced flow at the time of the survey, the weak thermocline that spanned the entire water column was a relic of the prior upwelling event.

METHODS

The 38 ft F/V *Bonnie Marietta*, owned and operated by Captain Mark Tognazzini of Morro Bay, served as the survey vessel on Monday, 12 March 2018. Douglas Coats of Marine Research Specialists (MRS) supervised scientific operations as Chief Scientist, and provided data-acquisition and navigational support during the survey. He also assisted with the deployment and recovery of the CTD and drifter, and he collected meteorological measurements at each station. Crewmember William Skok managed deck operations and measured Secchi depths at each station.

Auxiliary Measurements

Auxiliary measurements and observations were collected at each of the six stations after completion of the vertical profiling phase of the survey. Standard observations of weather and sea conditions, and beneficial uses, were augmented by visual inspection of the sea surface for floating particulates, oil sheens, and discoloration potentially related to effluent discharge. Other auxiliary measurements collected at each station included wind speeds and air temperatures measured with a handheld Holdpeak 866B Digital Thermo-Anemometer, and oceanic flow measurements made throughout the survey area using the aforementioned drogued drifter.

Additionally, at all six stations, a Secchi disk was lowered through the water column to determine its depth of disappearance. Secchi depths provide a visual measure of near-surface turbidity or water clarity. The depth of disappearance is inversely proportional to the average amount of organic and inorganic material suspended along a line of sight in the upper water column. As such, Secchi depths measure natural light penetration, which can be limited by increased suspended particulate loads from plankton blooms, onshore runoff, seafloor sediment resuspension, and wastewater discharge. They are also biologically meaningful because the depth of the euphotic zone, where most oceanic photosynthesis occurs, is limited to approximately twice the Secchi depth.

Instrumental Measurements

A Sea Bird Electronics SBE-19plusV2 Seacat CTD instrument package collected measurements of conductivity, temperature, light transmittance, dissolved oxygen (DO), pH, and pressure during the March 2018 survey. The six seawater properties used to assess receiving-water quality in this report were derived from the continuously recorded output from the CTD's probes and sensors. Although pressure-housing limitations confine the CTD to depths less than 680 m (Table 3), this is well beyond the maximum depth of the deepest station in the outfall survey. The entire CTD was returned to the factory in January 2015 for full calibration and servicing. The transmissometer and DO probe were returned to the manufacturer in January 2016 for further servicing, repair, and calibration.

Table 3. CTD Specifications

Component	Units	Range	Accuracy	Resolution
Housing (19p-1a; Acetron Plastic)	m	0 to 680	—	—
Pump (SBE 5P)	—	—	—	—
Pressure (19p-2h; Strain-Gauge)	dBar	0 to 680	±1.7	± 0.10
Conductivity	Siemens/m	0 to 9	± 0.0005	± 0.00005
Salinity	‰	0 to 58	± 0.004	± 0.0004
Temperature	ºC	–5 to 35	± 0.005	± 0.0001
Transmissivity (WETLabs C-Star)[13]	%	0 to 100	± 0.3	± 0.03
Oxygen (SBE 43)	% Saturation	0 to 120	± 2	—
pH (SBE 18)	pH	0 to 14	± 0.1	—

The precision and accuracy of the various probes, as reported in manufacturer's specifications, are listed in Table 3. Salinity (‰) was calculated from conductivity measurements reported in units of Siemens/m. Density was derived from contemporaneous temperature (°C) and salinity data, and was expressed as 1000 times the specific gravity minus one, which is a unit of sigma-T (σ_t).

Assessments of all three of the physical parameters (salinity, temperature, and density) helped determine the lateral extent of the effluent plume during the towing phase of the survey. Additionally, during the vertical-profiling phase, they quantified layering, or vertical stratification and stability of the water column, which determines the behavior and dynamics of the effluent as it mixes with seawater within and beyond the ZID. Data on the three remaining seawater properties, light transmittance (water clarity), hydrogen-ion concentration (acidity/alkalinity – pH), and dissolved oxygen (DO), further characterized the receiving waters, and were used to assess compliance with water-quality criteria. Light transmittance was measured as a percentage of the initial intensity of a transmitted beam of light detected at the opposite end of a 0.25-m path. Transmissivity readings are reported relative to 100% transmission in air, so the maximum theoretical transmission in (pure) water is expected to be 91.3%.

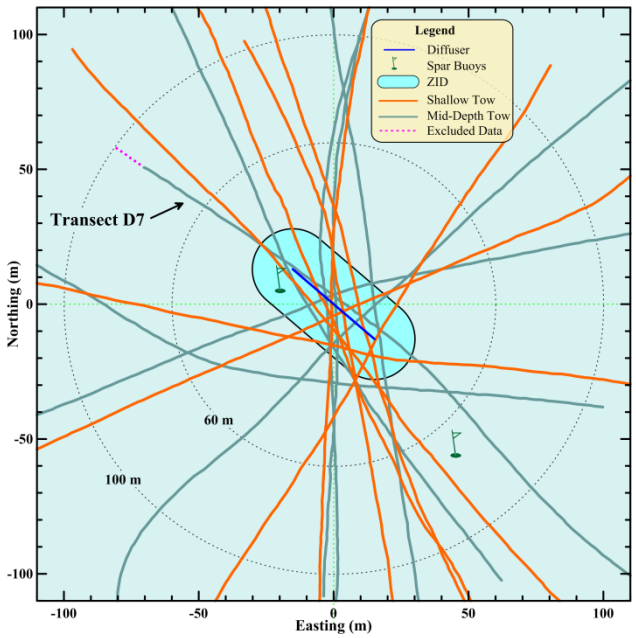

Figure 7. CTD Tracklines during the March 2018 Tow Surveys

Before beginning the mid-depth tow survey at 8:26 AM, the CTD was deployed beneath the sea surface for a fourteen-minute equilibration period as the vessel was positioned for the first transect. Prior to deployment, the CTD package had been configured for horizontal towing with forward-looking probes. The protective cage around the CTD was fitted with a horizontal stabilizer wing and a depth-suppression weight was added to the towline to achieve near constant-depth tows.

Eight transects of mid-depth data were collected at an average depth of 9.35 m and an average speed of 1.69 m/s over the span of 34 minutes (blue-green lines in Figure 7). Subsequently, at 9:02 AM, eight additional

[13] 25-cm path length of red (650 nm) light

passes were made with the CTD at an average depth of 1.5 m (orange lines). During this 32-minute shallow tow, vessel speed averaged 1.80 m/s.

At the observed towing speeds and the 4 Hz sampling rate, at least 2.2 CTD measurements were collected for each meter traversed. This complies with the NPDES discharge permit requirement for minimum horizontal resolution of at least one sample per meter during at least five passes around and across the ZID at two separate depths, one within the surface mixed layer and one at mid-depth within the thermocline. Contemporaneous navigation fixes recorded aboard the survey vessel were adjusted for CTD setback and aligned with time stamps on the internally recorded CTD data. The resulting data for the six seawater properties were then processed to produce horizontal maps within the upper and sub-thermocline portions of the water column.[14]

At 9:34 AM, following completion of the last shallow transect, the CTD package was brought aboard the survey vessel and reconfigured for vertical profiling. The CTD was redeployed at 9:44 AM, and was held beneath the surface for four minutes as the vessel was repositioned over Station RW1. The CTD was then raised to within 0.5 m of the sea surface and profiling commenced. The CTD was lowered at a continuous rate of speed to the seafloor. Measurements at all six stations were collected during a single deployment of the CTD package by towing it beneath the ocean surface while transiting between adjacent stations.

Quality Control

During the vertical-profiling and horizontal-towing phases of the survey, real-time data were monitored for completeness and range acceptability. Although real-time monitoring indicated that the recorded properties were complete and within acceptable coastal seawater ranges,[15] subsequent post-processing revealed events that impacted portions of the data, resulting in the adjustment or exclusion of these data prior to initiating the compliance analysis. As in prior surveys, review of the tow data revealed that the CTD changed depth when the vessel executed a turn at the end of each transect. These vertical offsets in CTD depth are introduced by changes in vessel speed and direction that are instituted to realign the vessel between each transect. Because of the complex interaction between turn radius, vessel speed, and CTD depth, the CTD's target depth cannot always be maintained at these times.

Because the discharge-related anomalies used for compliance analysis are identified by comparing the amplitudes of measurements acquired at the same depth level, the ability to resolve anomalies with statistical certainty is compromised when data from different depth levels are combined in the horizontal maps. This is particularly true when the water column is strongly stratified, but remains a concern even in the presence of weak stratification, as was the case during the March 2018 survey. However, only a small portion of Transect D7 exhibited an unacceptable depth offset due to vessel turning within the 100-m survey area (purple dotted line in Figure 7).

Additionally, the pH sensor experienced an unusually extended equilibration period that affected the accuracy of the raw CTD data collected during the first mid-depth tow transect (D1), and to a lesser extent, the initial portion of second transect (D2). The pre-survey soak period was too brief to provide full equilibration, and pH readings were artificially elevated during these two transects. Fortunately, the equilibration process produced a steady temporal decline in pH offset that could be accurately characterized by fitting an orthogonal polynomial to the pH time series from this initial portion of the mid-depth tow data.

[14] Figures 9 and 10 later in this report

[15] Field sampling protocols employed during the survey generally followed the field operations manual for the Southern California Bight Study (SCBFMC 2002), which includes CTD cast-acceptability ranges listed in Table 2 of the manual.

Temporal correction for pH equilibration and exclusion of small portions of data due to depth offset did not adversely affect the compliance analysis, however. The pH correction was small within the 100-m survey area, and the largest reduction of less than 0.19 pH units only occurred along the initial portion of Transect D1. Similarly, the small portion of excluded depth-offset data was located along the edge of the 100-m survey area, and the remaining transects were long enough to fully encompass the 100-m survey area surrounding the diffuser structure. Specifically, the tow data that was included in the compliance analysis, shown by the solid orange and blue-green lines in Figure 7, met the permit monitoring requirement of at least five passes near the diffuser structure at each tow depth.

RESULTS

The first-quarter receiving-water survey was conducted on the morning of Monday, 12 March 2018. The survey commenced at 8:13 AM with the deployment of the drogued drifter. Over the ensuing two hours and eight minutes, offshore observations and measurements were collected as required by the NPDES monitoring program. The survey ended at 10:21 AM with the retrieval of the drogued drifter. Collection of required visual observations of the sea surface was unencumbered throughout the survey.

Auxiliary Observations

On the morning of 12 March 2018, skies were partially overcast, with very light breeze out of the north that was almost imperceptible until the very end of the survey, when the auxiliary observations were collected (Table 4). Auxiliary observations were collected beginning at 10:12 AM, after completion of the vertical profiling phase of the survey. During the subsequent fourteen minutes, each station was re-occupied beginning with Station RW6. After auxiliary observations were collected at Station RW6, stations were sampled sequentially progressing toward the north. During that time, however, wind speed and air temperature increased perceptibly. A swell out of the northwest had a significant wave height of one-to-two feet. With average air temperatures between 19.5 and 21.8°C, the atmosphere was significantly warmer than the 12.7°C sea surface temperature.

Table 4. Standard Meteorological and Oceanographic Observations

	Location[16]		Diffuser Distance	Time	Air	Cloud Cover	Wind Avg	Wind Dir (from)	Swell Ht/Dir	Secchi Depth
Station	Latitude	Longitude	(m)	(PDT)	(°C)	(%)	(kt)	(°T)	(ft/°T)	(m)
RW1	35° 23.256' N	120° 52.497' W	95.2	10:26:03	21.8	30%	3.3	330	1-2 NW	14.0
RW2	35° 23.236' N	120° 52.508' W	56.3	10:24:02	21.0	40%	2.9	340	1-2 NW	10.0
RW3	35° 23.212' N	120° 52.504' W	18.8	10:21:13	20.5	40%	2.2	20	1-2 NW	10.5
RW4	35° 23.188' N	120° 52.501' W	12.0	10:18:28	20.5	40%	2.0	350	1-2 NW	10.5
RW5	35° 23.166' N	120° 52.500' W	48.2	10:16:13	20.9	45%	0.6	350	1-2 NW	10.5
RW6	35° 23.146' N	120° 52.501' W	85.7	10:12:03	19.5	50%	0.2	350	1-2 NW	10.5

There was no evidence of floating particulates, oil sheens, or any discoloration of the sea surface associated with the presence of wastewater constituents. The only visual indication of the discharge plume was a surface boil located directly over the diffuser structure. There was no other visual evidence of effluent, such as discoloration or floating particulates at or beneath the sea surface during the survey. Ambient light penetration beneath the sea surface was largely unencumbered throughout the water column during the March 2018 survey. Transmissivity was uniformly high throughout the water column, and reached levels near those of pure seawater within the lower half of the water column.

[16] Locations are the vessel positions at the time the Secchi depths were measured. These depart from the CTD profile locations listed in Table 2 because they were collected after completion of the CTD profiling.

During most surveys, upwelling-induced phytoplankton blooms limit light penetration within the upper half of the water column. Upwelling carries nutrients upward into the euphotic zone where they are assimilated by phytoplankton. This upwelling-driven primary production, in conjunction with population increases in the associated zooplanktonic herbivores, causes a sharp decrease in seawater transmissivity within the euphotic zone. During even mild upwelling conditions, the elevated planktonic densities reduce the transmittance of ambient light and typically reduce Secchi depths to around 4 m. Under those circumstances, the euphotic zone is restricted to the upper half of the water column (twice the Secchi depth) and no material amount of ambient light penetrates into the lower water column.

However, because the moderate upwelling conditions that prevailed in the weeks prior to the March 2018 survey had largely dissipated, a plankton-induced turbidity increase within the upper water column was scarcely measureable, and Secchi depths were unusually deep (Table 4). The euphotic zone reached the seafloor at all stations, and at Station RW1, the Secchi disk came within 2.5 m of the seafloor before it faded from view. The 14 m Secchi depth observed at that station was the deepest measured in at least a decade of MBCSD monitoring. That measurement documented the presence of a 28-m euphotic zone wherein ambient light easily penetrated to the seafloor. With Secchi depths equal to or exceeding 10 m at all stations, extraordinarily high levels of ambient light was illuminating the entire water column during the March 2018 Survey. This includes the ZID Stations RW3 and RW4, where the presence of dilute wastewater was observed within the upper water column as described in the *Instrument Observations* Section below.

However, there is no obvious explanation for the large spatial variation in Secchi depths recorded during the March 2018 Survey. As with the 14-m Secchi depth measured at the Upcoast Midfield Station RW1, the large 4-m range in Secchi depths among the stations was highly unusual in the historical database. Occasionally, in past surveys, entrainment of more- or less-turbid deep ambient seawater within the rising effluent plume resulted in slightly shallower or deeper Secchi depths at the ZID stations, but the differences were typically less than 1 m. Moreover, plume entrainment cannot account for the spatial distribution during the March 2018 survey because the stations where the plume signature was observed within the upper water column did not exhibit a significant departure from the 10.5-m median Secchi depth.

The last pertinent set of auxiliary observations assessed the quality of effluent that was being discharged around the time of the survey. Communication with plant personnel and subsequent review of effluent discharge properties around the time of the survey, confirmed that the treatment process was performing well. The 0.841 million gallons of effluent discharged on 12 March had a temperature of 19°C, a pH of 7.2, and a suspended-solids concentration of 31 mg/L. An effluent sample collected on 14 March, two days after the survey, had a biochemical oxygen demand (BOD) of 32 mg/L. No oil and grease was detected within an effluent sampled collected the day after the survey.

Instrumental Observations

Data collected during vertical profiling were processed in accordance with standard procedures (SCCWRP 2002), and are collated at 0.5-m depth intervals in Table 5. Data collected during the March 2018 survey reflect weakly stratified conditions within Estero Bay indicative of a relaxation in coastal upwelling following a pulse of upwelling wind of significant strength (refer to the inset in Figure 6). As described previously, upwelling of varying intensity occurs most of the year along the central California coast, with the strongest upwelling winds beginning in March or April and extending through the summer. The intensity of upwelling tends to decline into fall, although pulses of sustained northwesterly winds still occur. An intense upwelling event results in the rapid influx of dense, cold, saline water at depth and leads to a sharp thermocline, halocline, and pycnocline where temperature, salinity, and density change rapidly

Table 5. Vertical Profile Data Collected on 12 March 2018

Depth (m)	Temperature (°C)						Salinity (‰)					
	RW-1	RW-2	RW-3	RW-4	RW-5	RW-6	RW-1	RW-2	RW-3	RW-4	RW-5	RW-6
0.5		12.665	12.623	11.987	12.718	12.660		33.541	33.540	33.461	33.542	33.542
1.0	12.649	12.658	12.640	12.039	12.692	12.666	33.543	33.542	33.540	33.424	33.541	33.542
1.5	12.624	12.609	12.618	12.043	12.626	12.651	33.544	33.541	33.538	33.445	33.535	33.540
2.0	12.563	12.580	12.582	12.049	12.604	12.623	33.547	33.543	33.538	33.458	33.536	33.540
2.5	12.545	12.557	12.290	12.010	12.592	12.601	33.547	33.545	33.492	33.442	33.540	33.540
3.0	12.520	12.486	12.134	12.001	12.587	12.593	33.549	33.538	33.481	33.454	33.544	33.543
3.5	12.495	12.426	12.090	12.003	12.578	12.587	33.552	33.531	33.480	33.458	33.547	33.545
4.0	12.471	12.408	12.057	12.006	12.558	12.584	33.554	33.529	33.478	33.454	33.550	33.547
4.5	12.437	12.402	12.031	12.006	12.546	12.572	33.557	33.529	33.475	33.456	33.553	33.550
5.0	12.399	12.415	12.032	12.014	12.530	12.554	33.556	33.531	33.478	33.464	33.553	33.554
5.5	12.375	12.395	12.033	12.079	12.473	12.536	33.554	33.528	33.481	33.482	33.546	33.554
6.0	12.360	12.278	12.037	12.031	12.415	12.510	33.551	33.513	33.485	33.474	33.534	33.555
6.5	12.326	12.221	12.060	11.996	12.379	12.499	33.544	33.514	33.493	33.472	33.530	33.556
7.0	12.276	12.192	12.091	12.016	12.252	12.491	33.533	33.516	33.503	33.475	33.516	33.556
7.5	12.186	12.163	12.085	12.011	12.197	12.470	33.525	33.524	33.507	33.476	33.532	33.556
8.0	12.180	12.146	12.067	12.028	12.239	12.437	33.546	33.543	33.516	33.492	33.563	33.553
8.5	12.214	12.164	12.071	12.043	12.256	12.392	33.567	33.562	33.533	33.498	33.573	33.545
9.0	12.226	12.195	12.149	12.075	12.232	12.313	33.578	33.575	33.570	33.510	33.577	33.530
9.5	12.203	12.200	12.191	12.141	12.193	12.282	33.580	33.580	33.583	33.549	33.579	33.531
10.0	12.164	12.181	12.194	12.194	12.153	12.247	33.583	33.582	33.584	33.581	33.582	33.540
10.5	12.144	12.166	12.189	12.184	12.094	12.266	33.584	33.583	33.584	33.584	33.585	33.569
11.0	12.107	12.149	12.155	12.163	12.039	12.226	33.586	33.584	33.585	33.585	33.589	33.576
11.5	12.091	12.118	12.104	12.119	12.002	12.190	33.588	33.586	33.587	33.587	33.592	33.579
12.0	12.068	12.095	12.031	12.048	11.965	12.172	33.589	33.588	33.590	33.590	33.594	33.581
12.5	12.029	12.064	11.986	12.010	11.924	12.151	33.591	33.589	33.594	33.593	33.597	33.583
13.0	12.010	12.028	11.972	11.953	11.901	12.114	33.593	33.592	33.596	33.596	33.600	33.585
13.5	12.003	11.990	11.938	11.880	11.866	12.042	33.594	33.594	33.598	33.600	33.602	33.589
14.0	11.924	11.935	11.840	11.857	11.799	12.000	33.597	33.598	33.603	33.604	33.607	33.593
14.5	11.818	11.859	11.822	11.847	11.754	11.923	33.604	33.603	33.606	33.606	33.610	33.596
15.0	11.764	11.789	11.833	11.822	11.739	11.821	33.611	33.608	33.607	33.608	33.614	33.601
15.5	11.757	11.755	11.819	11.784	11.708	11.736	33.613	33.612	33.607	33.611	33.616	33.609
16.0	11.762	11.751	11.794	11.735	11.704	11.701	33.615	33.615	33.608	33.614	33.618	33.614
16.5			11.786	11.720	11.705	11.691			33.611	33.617	33.623	33.619

Table 5. Vertical Profile Data Collected on 12 March 2018 (continued)

Depth (m)	Density (σ_t)						pH					
	RW-1	RW-2	RW-3	RW-4	RW-5	RW-6	RW-1	RW-2	RW-3	RW-4	RW-5	RW-6
0.5		25.331	25.333	25.358	25.323	25.329		8.121	8.119	8.061	8.121	8.119
1.0	25.333	25.331	25.333	25.358	25.323	25.329	8.121	8.120	8.118	8.065	8.121	8.121
1.5	25.339	25.339	25.335	25.373	25.331	25.331	8.121	8.120	8.120	8.058	8.120	8.121
2.0	25.353	25.347	25.343	25.382	25.337	25.336	8.121	8.121	8.119	8.058	8.120	8.120
2.5	25.357	25.353	25.363	25.377	25.342	25.340	8.121	8.120	8.102	8.057	8.119	8.119
3.0	25.363	25.361	25.384	25.389	25.346	25.344	8.117	8.119	8.080	8.055	8.120	8.118
3.5	25.370	25.367	25.391	25.391	25.350	25.347	8.115	8.116	8.073	8.055	8.120	8.120
4.0	25.377	25.369	25.396	25.388	25.357	25.349	8.114	8.111	8.069	8.056	8.124	8.120
4.5	25.386	25.370	25.399	25.389	25.361	25.354	8.114	8.107	8.064	8.056	8.128	8.124
5.0	25.392	25.370	25.401	25.393	25.364	25.360	8.113	8.105	8.061	8.056	8.131	8.131
5.5	25.395	25.371	25.403	25.395	25.370	25.364	8.110	8.105	8.061	8.058	8.125	8.136
6.0	25.395	25.381	25.405	25.398	25.372	25.369	8.109	8.101	8.060	8.062	8.117	8.133
6.5	25.396	25.393	25.407	25.403	25.375	25.372	8.106	8.095	8.061	8.059	8.110	8.131
7.0	25.398	25.400	25.409	25.402	25.389	25.374	8.103	8.087	8.066	8.057	8.100	8.129
7.5	25.408	25.412	25.414	25.404	25.412	25.378	8.095	8.082	8.069	8.057	8.088	8.123
8.0	25.426	25.430	25.424	25.412	25.428	25.382	8.088	8.079	8.068	8.058	8.086	8.116
8.5	25.435	25.441	25.437	25.415	25.432	25.385	8.085	8.079	8.068	8.062	8.093	8.110
9.0	25.442	25.445	25.450	25.418	25.440	25.388	8.088	8.082	8.074	8.064	8.096	8.105
9.5	25.448	25.448	25.452	25.436	25.449	25.395	8.091	8.086	8.086	8.070	8.094	8.098
10.0	25.457	25.453	25.452	25.451	25.459	25.408	8.092	8.089	8.091	8.081	8.091	8.093
10.5	25.462	25.458	25.453	25.455	25.472	25.427	8.088	8.089	8.091	8.088	8.087	8.094
11.0	25.471	25.461	25.461	25.459	25.486	25.441	8.084	8.088	8.089	8.089	8.081	8.097
11.5	25.475	25.469	25.472	25.469	25.495	25.450	8.083	8.086	8.087	8.088	8.076	8.093
12.0	25.480	25.474	25.489	25.485	25.504	25.455	8.081	8.084	8.079	8.083	8.071	8.092
12.5	25.489	25.481	25.500	25.495	25.514	25.460	8.077	8.081	8.073	8.076	8.069	8.089
13.0	25.494	25.490	25.504	25.508	25.520	25.469	8.073	8.078	8.070	8.071	8.061	8.086
13.5	25.497	25.499	25.512	25.525	25.529	25.485	8.072	8.072	8.067	8.063	8.058	8.082
14.0	25.514	25.512	25.534	25.532	25.545	25.496	8.067	8.069	8.058	8.056	8.052	8.075
14.5	25.539	25.531	25.540	25.535	25.556	25.513	8.057	8.067	8.050	8.052	8.048	8.069
15.0	25.554	25.548	25.538	25.541	25.561	25.536	8.047	8.059	8.048	8.051	8.042	8.059
15.5	25.558	25.557	25.541	25.551	25.569	25.558	8.041	8.051	8.049	8.048	8.038	8.047
16.0	25.558	25.560	25.547	25.562	25.572	25.569	8.036	8.040	8.045	8.042	8.033	8.040
16.5			25.550	25.568	25.572	25.574			8.038	8.032	8.031	8.031

Table 5. Vertical Profile Data Collected on 12 March 2018 (continued)

Depth (m)	Dissolved Oxygen (mg/L)						Transmissivity (%)					
	RW-1	RW-2	RW-3	RW-4	RW-5	RW-6	RW-1	RW-2	RW-3	RW-4	RW-5	RW-6
0.5		8.573	8.584	7.453	8.573	8.564		92.785	91.741	92.348	93.379	92.851
1.0	8.510	8.530	8.514	7.453	8.562	8.562	92.926	92.906	91.683	92.204	93.217	92.152
1.5	8.443	8.507	8.375	7.429	8.560	8.552	92.898	92.591	91.806	92.089	92.781	92.188
2.0	8.439	8.448	7.723	7.356	8.537	8.544	92.983	92.314	91.807	92.441	91.949	91.859
2.5	8.359	8.268	7.579	7.373	8.522	8.519	92.840	92.042	91.664	92.465	91.412	91.419
3.0	8.313	8.191	7.559	7.366	8.505	8.510	92.295	91.972	91.942	92.710	91.243	91.121
3.5	8.266	8.174	7.485	7.371	8.512	8.510	92.468	92.151	92.460	92.534	91.191	90.913
4.0	8.214	8.177	7.445	7.378	8.503	8.531	93.102	92.340	92.405	92.569	91.587	91.081
4.5	8.141	8.214	7.452	7.436	8.416	8.555	93.855	92.368	92.836	92.592	91.869	92.249
5.0	8.093	8.080	7.455	7.524	8.217	8.504	93.812	92.477	92.956	92.770	93.148	92.948
5.5	8.067	7.825	7.481	7.360	8.144	8.449	93.645	92.408	93.007	92.698	93.655	93.887
6.0	7.985	7.787	7.556	7.354	8.012	8.428	93.773	92.181	92.894	92.664	93.201	94.096
6.5	7.908	7.726	7.574	7.391	7.766	8.368	93.570	92.461	92.854	92.583	92.958	94.232
7.0	7.748	7.688	7.524	7.380	7.823	8.234	93.597	92.980	93.008	92.759	92.928	94.418
7.5	7.751	7.674	7.514	7.436	7.934	8.173	93.047	93.198	92.995	92.887	93.308	93.911
8.0	7.832	7.749	7.616	7.470	7.927	8.093	93.475	93.725	93.281	93.168	93.714	93.169
8.5	7.879	7.802	7.770	7.574	7.856	7.933	94.458	94.149	93.581	92.996	94.624	92.674
9.0	7.805	7.802	7.798	7.755	7.763	7.910	94.630	94.881	93.987	93.378	94.830	93.106
9.5	7.721	7.759	7.794	7.776	7.672	7.894	95.607	95.331	94.787	94.188	95.217	93.551
10.0	7.674	7.722	7.758	7.743	7.558	7.917	95.544	94.860	95.395	95.352	95.526	93.719
10.5	7.617	7.701	7.684	7.705	7.484	7.815	95.618	95.314	95.513	95.801	95.641	94.332
11.0	7.602	7.616	7.539	7.590	7.439	7.777	95.278	95.691	95.555	95.755	95.768	95.696
11.5	7.524	7.597	7.452	7.482	7.362	7.744	95.228	95.634	95.878	95.870	95.654	95.540
12.0	7.449	7.529	7.409	7.442	7.276	7.688	95.344	95.718	95.769	95.898	95.829	95.693
12.5	7.444	7.455	7.361	7.306	7.240	7.590	95.557	95.903	95.707	95.895	96.077	95.841
13.0	7.417	7.380	7.223	7.190	7.143	7.490	95.487	95.760	96.037	96.068	95.923	95.893
13.5	7.251	7.242	7.108	7.175	7.042	7.419	95.561	95.595	95.868	95.884	95.910	95.973
14.0	7.048	7.176	7.133	7.153	6.973	7.234	95.474	95.603	95.868	95.751	95.872	95.909
14.5	6.981	7.025	7.119	7.088	6.949	7.058	95.913	95.652	95.623	95.892	95.788	96.043
15.0	6.960	6.964	7.051	6.988	6.864	6.947	95.710	95.715	95.499	95.763	95.820	95.859
15.5	6.957	6.932	6.988	6.857	6.819	6.872	95.418	95.529	95.433	95.690	95.753	95.817
16.0	7.008	6.948	6.997	6.858	6.830	6.849	95.421	95.167	95.605	94.950	95.513	95.685
16.5			7.001	6.901	6.823	6.874			95.410	95.046	95.458	95.713

over a small vertical distance. Under these highly stratified conditions, isotherms crowd together to form a density interface that inhibits the vertical exchange of nutrients and other water properties, traps the effluent plume at depth, and reduces the initial dilution of the effluent plume.

If the upwelling winds are only of moderate strength, occur only briefly, or have not occurred recently; then vertical mixing slowly erodes the sharp contrast between the surface and deep watermasses. As a result, stratification appears as a more gradual vertical change in seawater properties that can eventually extend throughout the entire water column. This was the case for the March 2018 survey, namely, vertical mixing had completely eroded the sharply defined thermocline generated by the prior upwelling event. The remnants of the original upwelling-induced vertical interface appear as weak vertical gradients that extend throughout the water column at stations unaffected by the discharge (Stations RW1, RW5, and RW6 in Figure 8aef). The profiles at those stations reflect the ambient stratification present at the time of the survey. The profiles reveal that nearly all seawater properties steadily changed with depth throughout the entire water column, although a slight mid-depth perturbation is apparent in the profiles. Overall, however, the diffuse vertical transition that extended throughout the water column was composed of eroded remnants from the sharply defined mid-depth thermocline generated by the upwelling event in the weeks prior to the survey.

Regardless of the upwelling-event intensity, or the lapse in time since the event, regional upwelling events produce predicable vertical trends in seawater properties within the survey area. Namely, most seawater properties exhibit regularly increasing or decreasing values with depth that are determined by well-established physicochemical processes within ocean waters. These processes are evident in the seawater-property trends shown in Figures 8aef, and to some extent at Station RW2 in Figure 8b, even though intense upwelling winds had completely subsided by the time the survey was conducted. Specifically, temperature (red line), DO (dark blue line), and pH (olive-colored line) steadily decrease with depth. These decreases are mirrored by density, salinity, and transmissivity profiles (black, light green, and light blue lines) that generally increase with depth.

Thus, the water-property distribution throughout the water column constitutes a gradual transition from warm well-oxygenated sea-surface conditions to dissimilar conditions associated with a distinct watermass that was present near the seafloor. The seafloor watermass migrated shoreward along the seafloor as part of the upwelling process and carried cold, nutrient-rich but oxygen-poor seawater that reflect conditions typical of its origin deep offshore. Within the survey area, the remnants of this deep offshore watermass are most apparent below 14 m. This 2-m thick bottom layer contained seawater that was perceptibly colder and denser than shallow waters. As a result, temperatures decrease (red line) and density increases (black line) with increasing depth within the overlying transition zone (Figures 8abef). Similarly, the deep watermass had not been in recent direct contact with the atmosphere, and biotic respiration and decomposition had depleted its DO levels (dark blue line). Biotic respiration and decomposition also produces carbon dioxide (CO_2), and in its dissolved state, the increased concentration of carbonic acid appears as a concomitant reduction in pH (olive-colored line) near the seafloor. Lastly, seawater properties within this deep watermass originate within the northward-flowing Davidson undercurrent that carries saline waters out of the Southern California Bight and northward along the central California coast. As result of its presence at depth, salinity (light green line) tends to increase with increasing depth.

Although these well-established trends in seawater properties were readily apparent during the March 2018 survey, the magnitudes of the vertical gradients were small compared to other surveys conducted during upwelling events. These gradual trends reflect a water column that was only weakly stratified at the time of the March 2018 survey. This weak stratification profoundly affected the dynamics of effluent dispersion. Specifically, during most other surveys, when the water column was strongly stratified by

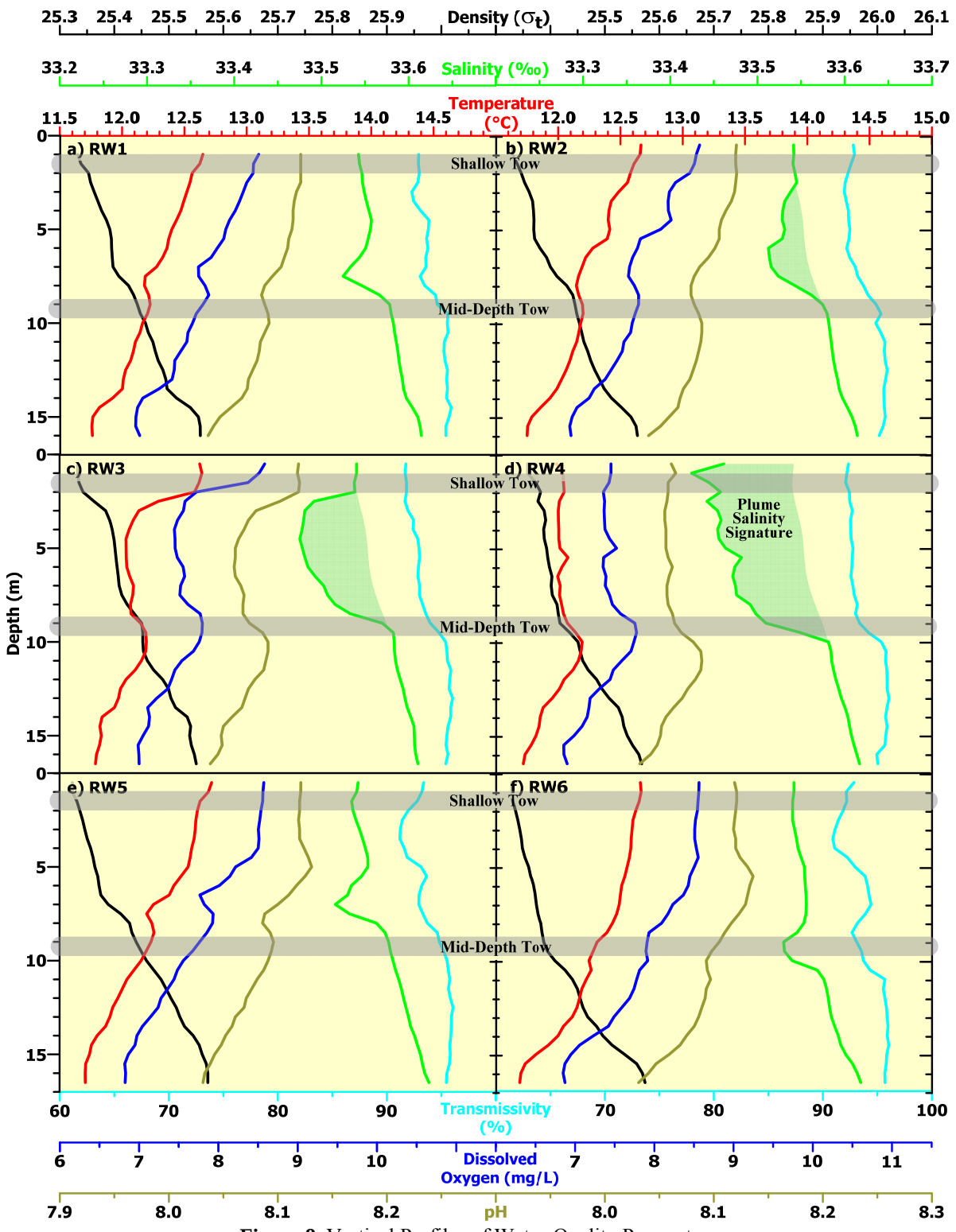

Figure 8. Vertical Profiles of Water-Quality Parameters

recent upwelling, the rising plume became trapped at depth within the water column, thereby limiting its full capacity for dilution. In contrast, during the March 2018 survey, the plume not only rose all the way to the sea surface, but also did so with such upward momentum that it actually formed a visually apparent boil on the sea surface. The surface signature of the effluent plume was also unmistakably confirmed by marked salinity reductions in sea-surface salinity at Downcoast ZID Station RW4 (refer to the green shading that extends throughout the upper half of the water column in Figure 8d). Additionally, at that station, the gradual vertical gradients seen in other water properties within the upper half of the ambient water column at other stations (Figure 8aef), were largely eliminated by the rising effluent plume. Specifically, entrainment and upward transport of deep ambient seawater within the rising plume produced nearly uniform seawater properties throughout the upper water column as Station RW4.

The low-salinity signature of dilute wastewater constituents was also apparent at the Upcoast ZID and Nearfield Stations RW3 and RW4 (Figure 8bc). However, at those locations, the low-salinity signature did not extend all the way to the sea surface, but remained submerged beneath 2 m. At Station RW3, where the plume signature extended from 2 m to 9 m (green shading in Figure 8c), other seawater properties also exhibited vertically uniform temperatures, DO, and pH (red, dark blue, and gold lines) comparable with those found in ambient seawater at depth. However, because the plume remained submerged just beneath the sea surface, the deep seawater properties entrained within the plume formed a sharp vertical contrast with ambient seawater properties at the sea surface.

The horizontal maps in Figures 9 and 10 lend additional important insight into the buoyancy dynamics of the effluent plume. They document how the plume initially rose through the water column and impinged on the sea surface, but then subsequently sank slightly as it was transported toward the north. Because of the ambient water column's relatively weak stratification at the time of the March 2018 survey, the plume's rapid rise through the water column was captured during the mid-depth tow. At a depth near 9 m, localized entrainment-generated anomalies coincide spatially with the plume's low-salinity signature (Figure 9b). Slightly reductions in temperature, density, transmissivity, DO, and pH were generally restricted to the ZID, although some transport toward the east-northeast was also evident (Figure 9acdef). The negative density anomaly (Figure 9c) demonstrates that the plume was buoyant at that depth, and would continue to rise within the water column before completion of the initial dilution process.

In contrast, the shallow tow captured the plume signature near the completion of the initial dilution process (Figure 10). Anomalies in all seawater properties (Figure 10acef) other than transmissivity (Figure 10d) coincided spatially with the plume's low-salinity signature (Figure 10a). However, in contrast to the negative density anomaly delineated in the deep tow, density within the shallow-tow signature was greater than the surrounding seawater (note the scale reversal in Figure 9c). This reveals that the plume was negatively buoyant at that depth. Thus, the shallow tow captured the signature of a plume whose upward momentum had caused it to overshoot its buoyant equilibrium depth and reach the sea surface within a limited area directly over the diffuser structure. Subsequently, the negatively buoyant plume would be expected to sink within the water column and accordingly, the vertical profiles at Stations RW2 and RW3 show that the plume had settled below 2 m (compare the green shading in Figure 8bc with the thick shaded horizontal line representing the shallow tow depth). Because the shallow tow was conducted at a depth of 1.5 m and above the plume's equilibrium depth, the plume's presence north of the diffuser structure was not captured in the shallow-tow maps (Figure 10).

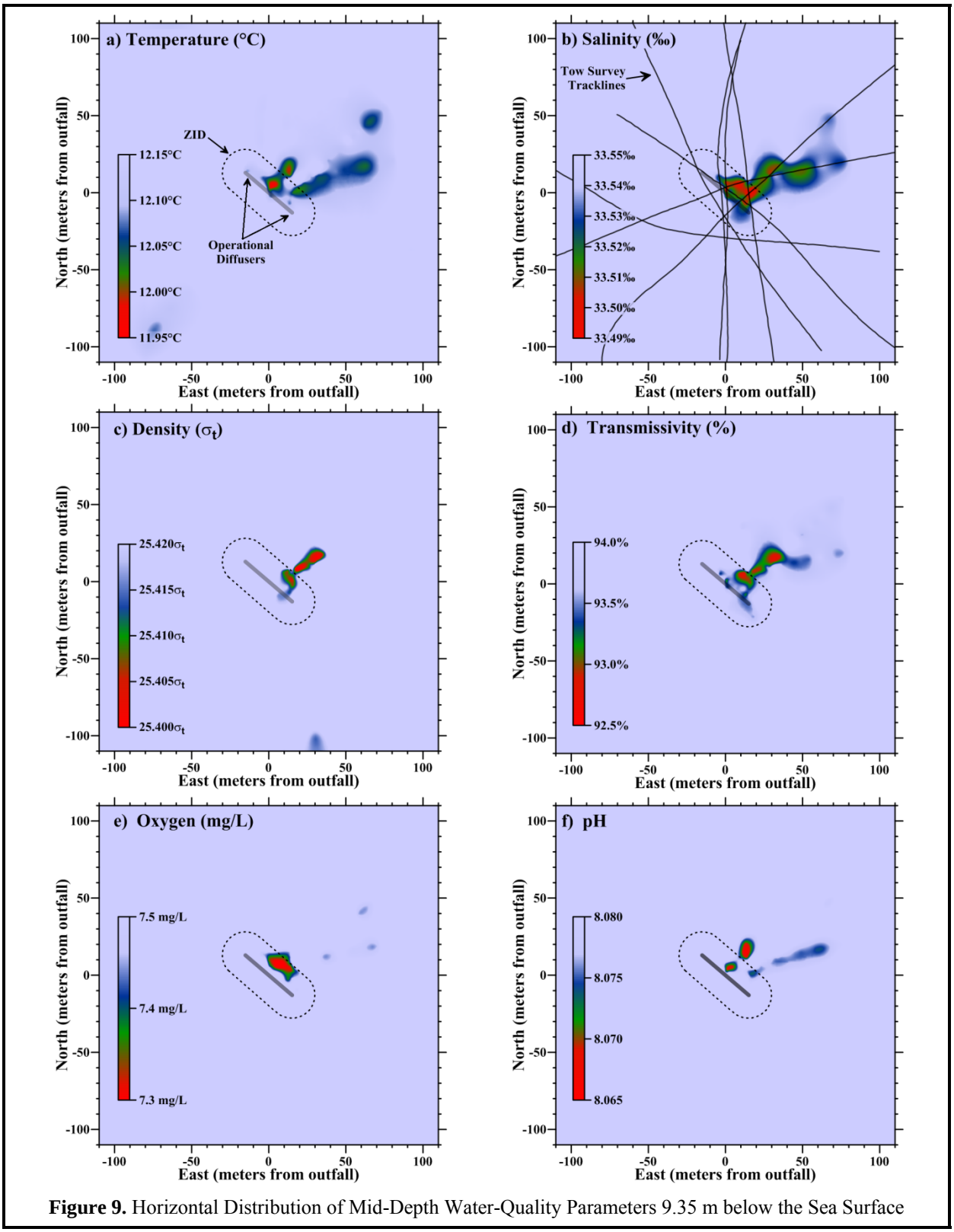

Figure 9. Horizontal Distribution of Mid-Depth Water-Quality Parameters 9.35 m below the Sea Surface

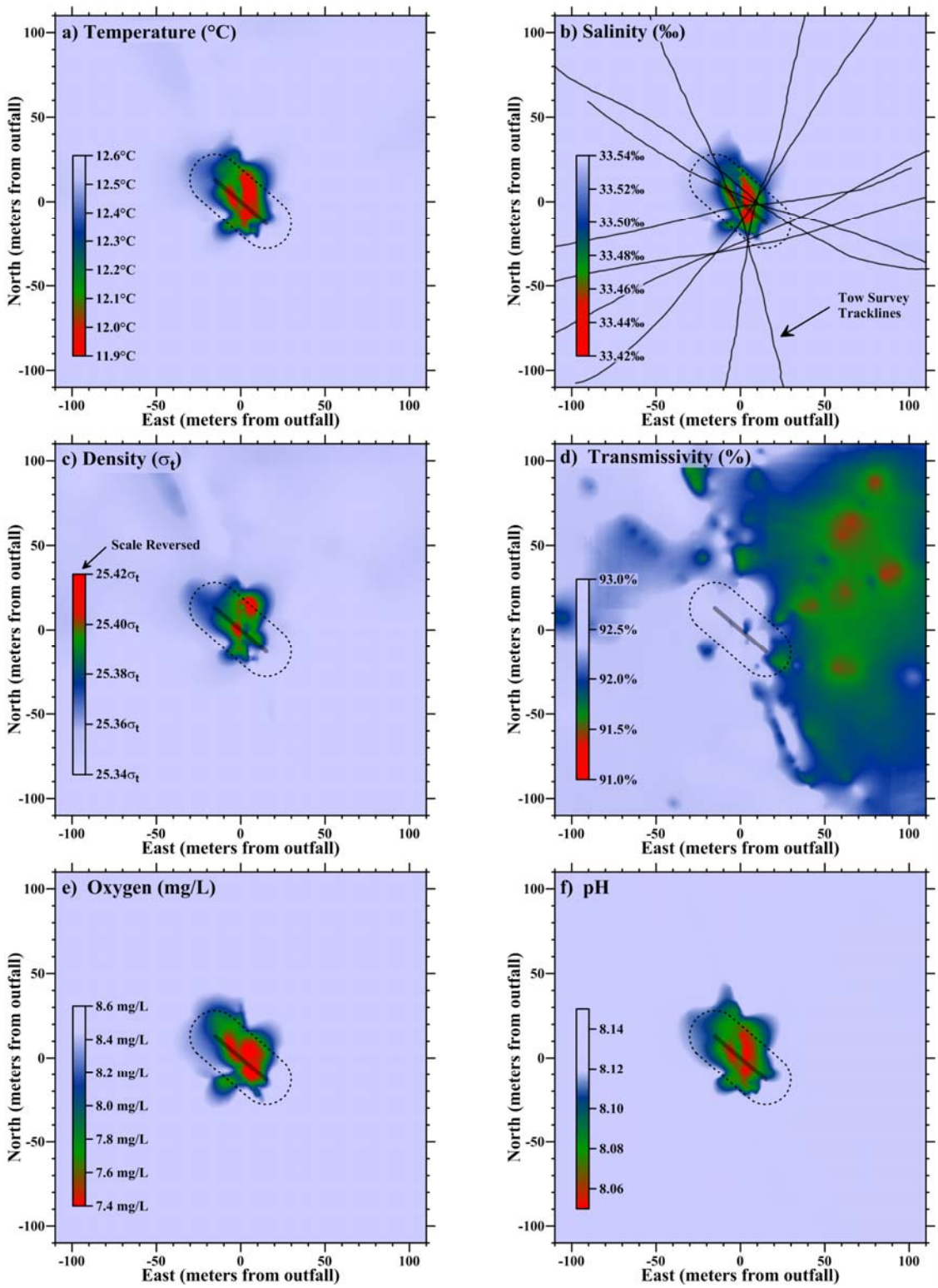

Figure 10. Horizontal Distribution of Shallow Water-Quality Parameters 1.5 m below the Sea Surface

All the seawater properties exhibited anomalies that clearly delineated the plume's lateral extent as it rose through the water column and impinged on the sea surface (Figures 8, 9,and 10). However, only the excursions in salinity and density resulted from the presence of dilute wastewater constituents. As described previously, the lateral anomalies in the other seawater properties arose from the entrainment of deep ambient seawater shortly after discharge. These deep seawater properties became apparent as a signature of the buoyant effluent plume when they were juxtaposed against the ambient seawater characteristics in the mid and upper water column. Because entrainment anomalies are generated by the physical movement of ambient seawater rather than the plume-dilution processes, they can be particularly long lived and remain apparent well after the wastewater constituents have dispersed far beyond recognition.

In addition to their longevity, entrainment-generated anomalies are only apparent when the water column is sufficiently stratified to cause a perceptible contrast between the shallow and deep ambient seawater within the rising plume. Only then does the initial dilution process produce entrainment anomalies. Initial dilution begins with intense mixing that is driven by the momentum of the effluent's ejection from the individual diffuser ports. Subsequent turbulent mixing caused by the plume's ascent through the water column is less intense, and as a result, the dilute effluent plume tends to retain the ambient seawater properties it acquired near the seafloor. However, such anomalies are irrelevant to the receiving-water compliance assessment because the permit restricts attention to water-quality changes caused solely by the presence of wastewater constituents rather than by a simple relocation of ambient seawater.

Outfall Performance

The efficacy of the outfall can be evaluated through a comparison of dilution levels measured at the time of the March 2018 survey, and dilutions anticipated from modeling studies that were codified in the discharge permit through limits imposed on effluent constituents. Specifically, the critical initial dilution applicable to the MBCSD outfall was conservatively estimated to be 133:1 (Tetra Tech 1992). That is, dispersion modeling estimated that, at the conclusion of the minimum expected initial mixing, 133 parts of ambient seawater would have mixed with each part of wastewater.

The 133:1 dilution estimate was based on worst-case modeling under highly stratified conditions, where trapping of the plume below a strong thermocline would curtail the additional buoyant mixing normally experienced during the plume's ascent through the entire water column. Additionally, the modeling assumed quiescent oceanic flow conditions, thereby restricting initial mixing processes to the ZID. Under those conditions, the modeling predicted that a 133:1 dilution would be achieved after the plume rose only 9 m from the seafloor, whereupon it would become trapped, ceasing to ascend farther in the water column. At that point, the plume would spread laterally with dilution occurring at a much-reduced rate. A 9-m ascent at the MBCSD outfall translates into a trapping depth that is 6.2 m below the sea surface. As described below, however, the lowest dilution levels observed during the March 2018 survey were much higher than the 133:1 predicted by the modeling, even though they were measured within the ZID, at greater depth, and well before the completion of the initial dilution process.

The conservative nature of the critical initial dilution determined from the modeling is an important consideration because it was used to specify permit limitations on chemical concentrations within wastewater discharged from the treatment plant. These end-of-pipe effluent limitations were back calculated from the receiving-water objectives in the COP (SWRCB 2005) using the projected 133-fold dilution determined from the modeling. Application of a higher critical dilution would relax the stringent end-of-pipe effluent limitations thought necessary to achieve the COP objectives after initial dilution is complete.

End-of-pipe limitations on contaminant concentrations within discharged wastewater were based on the definition of dilution (Fischer et al. 1979). From the mass-balance of a conservative tracer, the concentration of a particular chemical constituent within effluent before discharge (C_e) can be determined from Equation 1.

$$C_e \equiv C_o + D(C_o - C_s) \qquad \text{Equation 1}$$

where: C_e = the concentration of a constituent in the effluent,
C_o = the concentration of the constituent in the ocean after dilution by D (i.e., the COP receiving-water objective),
D = the dilution expressed as the volumetric ratio of seawater mixed with effluent, and
C_s = the background concentration of the constituent in ambient seawater.

By rearranging Equation 1, the actual dilution achieved by the outfall can be determined from measured seawater anomalies. This measured dilution can then be compared with the critical dilution factor determined from modeling. Salinity is an especially useful tracer because it directly reflects the magnitude of ongoing dilution. The regions of slightly reduced salinity apparent above the outfall in both tow-survey maps (Figures 9b and 10b), and in the vertical profiles measured at three of the stations (green shading in Figure 8bcd) were induced by the presence of dilute wastewater. These salinity anomalies document mixing processes within the effluent plume shortly after discharge, and as it rose through the water column, reached the sea surface, and then descended to its equilibrium depth where began to spread laterally.

The amplitudes of these salinity anomalies quantify the magnitude of wastewater dilution at the various stages of the initial mixing process. By rearranging Equation 1, the dilution ratio (D) can be computed from the salinity anomaly ($A = C_o - C_s$) as:

$$D \equiv \frac{(C_e - C_o)}{(C_o - C_s)} \propto -A^{-1} \qquad \text{Equation 2}$$

The salinity concentration within MBCSD effluent (C_e)[17] is small compared to that of the receiving seawater and, after dilution by more than 133 fold, the salinity of the effluent-seawater mixture is close to ambient salinity. Consequently, to a close approximation, dilution levels are inversely proportional to the amplitude of the salinity anomaly. Thus, a lower effluent dilution at a given location within the effluent plume is directly mirrored by a larger reduction in the measured salinity relative to that of the surrounding seawater.

Among the 11,033 CTD measurements collected during the March 2018 survey, the greatest reduction in salinity (-0.119‰) was recorded during the eighth transect of the shallow tow survey when a salinity of 33.421‰ was encountered only 1.5 m laterally from the diffuser structure and at a depth of 1.4 m below the sea surface (red shading in Figure 10b). From Equation 2, this salinity anomaly corresponds to a dilution of 272 fold (small patch of red immediately south of the diffuser structure in Figure 11 on the following page). The plume continued to mix as it was transported northward to Station RW3 and descended to its equilibrium depth below 2 m (green shading in Figure 8c). At that point, the initial dilution process was complete, and wastewater had been diluted by at least 322-fold.

[17] Wastewater samples have an average salinity of 0.995‰.

The shallow measured dilutions were comparable to the lowest dilution of 359-fold measured during the mid-depth tow (red shading in Figure 12). As with the shallow dilution determinations, the lowest mid-depth dilution was measured well within the ZID, and only 1.4 m laterally from the diffuser structure. However, because it was measured at a depth of 9.4 m and earlier in the initial mixing process, a lower dilution would have been expected. Instead, at that depth, it is likely that the mid-depth transects happened to miss the highly localized center of the rapidly rising plume.

Overall, these dilution measurements demonstrate that, during the March 2018 survey, the outfall was performing better than designed and was rapidly entraining seawater shortly after discharge. This resulted in dilution levels exceeding 272 fold before the initial dilution process was complete. These minimum measured dilutions were double the 133:1 dilution predicted by the worst-case modeling study, even though they were measured before the plume had settled into its equilibrium depth and completed the initial dilution process.

Upon completion of the initial dilution process, measured dilutions were 2.4-times the model's 133:1 critical initial dilution that was used to establish end-of-pipe permit limitations on contaminant concentrations within wastewater discharged from the MBCSD treatment plant. This demonstrates that, during the March 2018 survey, the COP receiving-water objectives were being easily met by the limits on chemical concentrations within discharged wastewater that are promulgated by the NPDES discharge permit issued to the MBCSD.

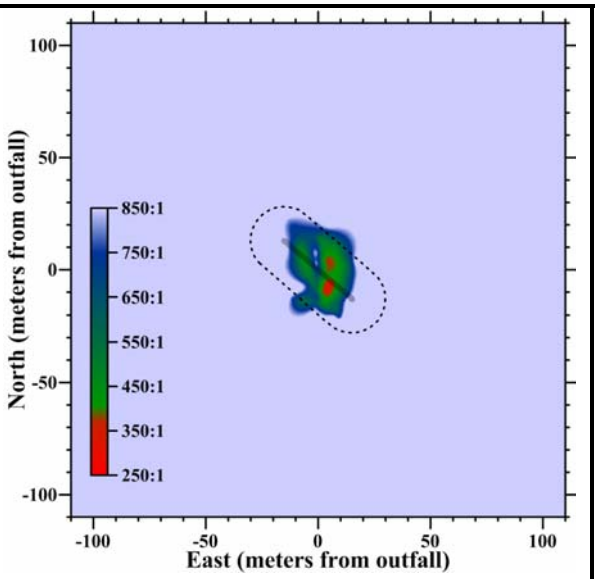

Figure 11. Shallow Plume Dilution Computed from Salinity Anomalies in Figure 10b

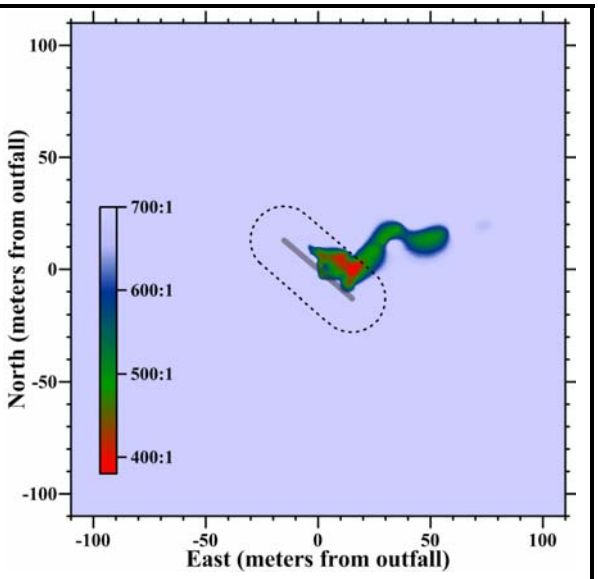

Figure 12. Mid-Depth Plume Dilution Computed from Salinity Anomalies in Figure 9b

COMPLIANCE

This section evaluates compliance with the water-quality limitations listed in the NPDES permit (Table 6 on the following page). The limits themselves are based on criteria in the COP, the Central Coast Basin Plan, and other state and federal policies that were designed to protect marine life and beneficial uses of ocean waters. Because the limits only pertain to changes in water properties that are caused by the presence of wastewater constituents beyond the ZID, instrumental measurements undergo a series of screening procedures prior to numeric comparison with the permit thresholds. Specifically, the quantitative analyses described in this section focus on water-property excursions caused by the presence of wastewater constituents beyond the ZID, whose amplitudes can be reliably discerned against the

Table 6. Permit Provisions Addressed by the Offshore Receiving-Water Surveys

Limit #	Limit
P1	Floating particles or oil and grease to be visible on the ocean surface
P2	Aesthetically undesirable discoloration of the ocean surface
P3	Temperature of the receiving water to adversely affect beneficial uses
P4	Significant reduction in the transmittance of natural light at any point outside the ZID
P5	The DO concentration outside the zone of initial dilution to fall below 5.0 mg/L or to be depressed more than 10% from that which occurs naturally
P6	The pH outside the zone of initial dilution to be depressed below 7.0, raised above 8.3, or changed more than 0.2 units from that which occurs naturally

backdrop of ambient fluctuations. A detailed understanding of ambient seawater properties, and their natural variability within the region surrounding the outfall, is therefore an integral part of the compliance evaluation presented in this section.

The results of the analyses performed on the March 2018 data demonstrate that the MBCSD discharge complied with the NPDES discharge permit. Moreover, although observations within the ZID are not subject to compliance evaluations, they met the prescribed limits because actual dilution levels routinely exceeded the conservative design specifications assumed in the discharge permit. Thus, the quantitative evaluation described in this section documents an outfall and treatment process that was performing at a high level during the March 2018 survey.

Permit Provisions

The offshore receiving-water surveys are designed to assess compliance with objectives dealing with undesirable alterations to six physical and chemical characteristics of seawater. Specifically, the permit states that wastewater constituents within the discharge shall not cause the limits listed in Table 6 to be exceeded.

The first two receiving-water limits, P1 and P2, rely on qualitative visual observations for compliance evaluation. Compliance was demonstrated during the March 2018 survey through visual inspection of the sea surface that documented an absence of floating wastewater materials, oil, grease, and discoloration.

Compliance with the remaining four receiving-water limitations was quantitatively evaluated through a comparison between instrumental measurements and numerical limits listed in the NPDES permit. For example, in P5 and P6, the fixed numeric limits on absolute values of DO (>5 mg/L) and pH (7.0 to 8.3) can be directly compared with field measurements within the dilute wastewater plume beyond the ZID. However, both P5 and P6 also contain narrative limits, which originate within the COP, and define unacceptable water-quality impacts in terms of "*significant*" excursions beyond those that occur "*naturally*." Quantitative evaluation of these limits requires a further comparison of field measurements with numerical thresholds that reflect the natural variation in temperature, transmissivity, DO, and pH within the receiving waters surrounding the outfall.

As described in prior sections, natural variation in seawater properties can result from a variety of oceanographic processes. These processes establish the range in ambient seawater properties caused by natural spatial variation within the survey region at a given time (e.g., vertical stratification), and by temporal variations caused by seasonal and interannual influences (e.g., El Niño and La Niña). Of particular interest are upwelling and downwelling processes that not only determine average properties at a given time, but also the degree of water-column stratification, or spatial variability, present during any given survey.

Screening of Measurements

Accurately evaluating whether any of the 11,033 CTD measurements collected during the March 2018 survey exceeded a permit limit can be a complicated process. For example, although apparently significant excursions in an individual seawater property may be related to the presence of wastewater constituents, they may also result from instrumental errors, natural processes, entrainment of ambient bottom water in the rising effluent plume, statistical uncertainty, ongoing initial mixing within and beyond the ZID, or other anthropogenic influences (e.g., dredging discharges or oil spills).

Because of this complexity, measurements were first screened to determine whether numerical limits on individual seawater properties even pertain (Table 7). The screening procedure sequentially applies three questions to restrict attention to: 1) the oceanic area where permit provisions pertain; 2) changes due to the presence of wastewater constituents; and 3) changes large enough to be reliably detected against the backdrop of natural variation. The measurements that remain after completing the screening process can then be compared with Basin-Plan numerical limits and COP allowances.

Table 7. Receiving-Water Measurements Screened for Compliance Evaluation

Topic Addressed	Screening Question	Answer		
		No	**Yes[18]**	***Parameter***
Location	1. Was the measurement collected beyond the 15.2-m ZID boundary where modeling assumes that initial dilution is complete?	*1,550*	*9,483*	All
Wastewater Constituents	2. Did the beyond-ZID measurement coincide with a quantifiable salinity anomaly (≤550:1 dilution level) indicating the presence of detectable wastewater constituents?	*9,375*	*108*	All
Natural Variation	3. Did seawater properties associated with the wastewater measurements depart significantly from the expected range in ambient seawater properties at the time of the survey?	*108*	*0*	Temperature
		108	*0*	Transmissivity
		108	*0*	DO
		108	*0*	pH

The subsection following this one provides additional lines-of-evidence that demonstrate compliance with numerical permit limits independent of the screening process. The rationale for identifying observations suitable for further compliance analysis is presented in the following descriptions of the three screening steps.

1. Measurement Location: The COP states that compliance with its receiving-water objectives "*shall be determined from samples collected at stations representative of the area within the waste field where initial dilution is completed.*" Initial dilution includes the mixing that occurs from the turbulence associated with both the ejection jet, and the buoyant plume's subsequent ascent through the water column.

Although currents often transport the plume well beyond the ZID before the initial dilution process is complete, the COP states that dilution estimates shall be based on "*the assumption that no currents, of sufficient strength to influence the initial dilution process, flow across the discharge structure.*" Because of this, the regulatory mixing distance, which is equal to the 15.2-m water depth of the discharge, provides a conservative boundary to screen receiving-water data for subsequent compliance evaluation. Application of this initial screening question to the March 2018 dataset eliminated 1,550 of the original 11,033 receiving-water observations from further consideration because they were collected within the

[18] Number of remaining CTD observations of potential compliance interest based on sequential application of each successive screening question

ZID (Table 7, Question 1). The remaining 9,483 observations were carried forward in the screening analysis.

2. Presence of Wastewater Constituents: The MBCSD discharge permit restricts application of the numerical receiving-water limits to excursions caused by the presence of wastewater constituents. This confines the compliance analysis to changes caused "*as the result of the discharge of waste*," as specified in the COP, rather than anomalies that arise from the upward movement of ambient seawater entrained within the buoyant effluent plume. Analyses conducted on quarterly receiving-water surveys over the last decade have demonstrated that the direct influence of dilute wastewater is almost never observed in any seawater property other than salinity, except very close (<1 m) to a diffuser port and within its ejection jet.

In fact, negative salinity anomalies are the only consistent indicator of the presence of wastewater constituents within receiving waters. Wastewater salinity is negligible compared to that of the receiving seawater, so the presence of a distinct salinity minimum provides *de facto* evidence of the presence of wastewater constituents. Because of the large contrast between the nearly fresh wastewater and the salty receiving water, salinity provides a powerful tracer of dilute wastewater that is unrivaled by other seawater properties. Other properties do not exhibit such a large contrast and, as such, their wastewater signatures dissipate rapidly upon discharge with very little mixing. Wastewater's lack of salinity, however, provides a definitive tracer that allows the presence of effluent constituents to be identified even after dilution many times greater than the 133-fold critical initial dilution assumed in the discharge permit.

As described in the previous section, wastewater-induced reductions in salinity can be used to determine the amount of dilution achieved by initial mixing. Based on statistical analyses of the natural variability in salinity readings measured near the outfall over a five-year period between 2004 and 2008, the smallest reduction in salinity that can be reliability detected within receiving waters is 0.062‰. This represents a dilution level of 542 fold in Equation 2. Salinity reductions that are smaller than 0.062‰ cannot be consistently discerned against the backdrop of natural variation, and would not result in discernible changes in other seawater properties. Eliminating those measurements from further evaluation restricts attention to excursions in temperature, light transmittance, DO, and pH that are potentially related to the presence of wastewater constituents.

As discussed previously, the greatest salinity reductions observed during the March 2018 survey were recorded directly over the outfall during the mid-depth and shallow tow surveys, and near the sea surface at Downcoast ZID Station RW4. Although only a moderate oceanic current prevailed at the time of the survey, portions of the spreading subsurface plume were carried well beyond the ZID to Upcoast Nearfield Station RW2 (Figure 8b) at the conclusion of the initial dilution process. As a result, a number of quantifiable salinity reductions were measured well outside the ZID boundary. Even though some of these 108 salinity anomalies were clearly measured prior to completion of the initial dilution process, they were outside the ZID and reliably associated with the presence of wastewater constituents (Table 7). The remaining 9,375 salinity measurements collected beyond the ZID during the March 2018 survey did not have salinity reductions that were larger than the 0.062‰ plume-detection threshold, and therefore would not have contained effluent that had been diluted by less than 550-fold.

3. Natural Variation: An integral part of the compliance analysis is determining whether a particular anomalous measurement resulted from the presence of wastewater constituents, or whether it simply became apparent because ambient seawater was relocated (upward) by the plume. If the measurement does not significantly depart from the natural range in ambient seawater properties at the time of the survey, then it is inappropriate to ascribe the departure to the presence of wastewater constituents. Thus,

quantifying the natural variability around the outfall at the time of the survey is necessary for determining whether a particular observation warrants comparison with the numeric permit limits.

A statistical analysis of receiving-water data collected around the outfall was used to establish the range in natural conditions within the survey area (first three data columns of Table 8). These ambient-variability ranges were used to identify significant departures from natural conditions that could be indicative of adverse discharge-related effects on water quality. The same five-year database used to establish the within-survey salinity variation discussed previously, was also used to establish one-sided 95% confidence bounds on transmissivity (-10.2%), temperature (+0.82°C), DO (-1.38 mg/L), and pH (± 0.094). These were combined with 95th percentiles determined from the March 2018 ambient seawater data, to establish time-specific natural-variability thresholds in a manner analogous to COP Appendix VI. The percentiles were determined from March-2018 vertical profile data collected largely at Stations RW1, RW5, and RW6, and excluded measurements potentially affected by the discharge at other stations.

Table 8. Compliance Thresholds

Water Quality Property	95% Confidence Bound[19]	95th Percentile[20,21]	Natural Variability Threshold[22]	COP Allowance[23]	Basin Plan Limit[24]	Extremum[25]
Temperature (ºC)	0.82	12.64	>13.46	>15.66	—	≤12.72
Transmissivity (%)	-10.2	91.7	<81.5	—	—	≥90.9
DO (mg/L)	-1.38	6.88	<5.50	<4.95	<5.00	≥6.82
pH (minimum)	-0.094	8.040	<7.946	<7.746	<7.000	≥8.031
pH (maximum)	0.094	8.124	>8.218	>8.418	>8.300	≤8.148

Temperature, transmissivity, pH, and DO concentrations associated with the 108 remaining measurements of potential compliance interest were all well within their respective ranges of natural variability (Table 7, Question 3). As such, the screening process unequivocally eliminated all of the measurements collected during the March 2018 survey from further consideration in the compliance analysis. In fact, all of the documented excursions in these properties were the result of physical processes unrelated to the presence of wastewater constituents, namely, entrainment of near-bottom seawater within the rising effluent plume.

[19] The one-sided confidence bound measures the ability to reliably determine ambient seawater properties within surveys as a whole. They were determined from an analysis of the variability in ambient water-quality data collected during 20 quarterly surveys conducted between 2004 and 2008. Although water-quality observations potentially affected by the presence of wastewater constituents were excluded from the analysis, more than 9,200 remaining observations for each of the six seawater properties accurately quantified the inherent uncertainty in defining the range in natural conditions.

[20] The COP (Appendix I, Page 27, SWRCB 2005) defines a "*significant*" difference as "*a statistically significant difference in the means of two distributions of sampling results at the 95% confidence level*." Accordingly, COP effluent analyses (Step 9 in Appendix VI, Page 42, Ibid.) are based "*the one-sided, upper 95% confidence bound for the 95th percentile*."

[21] The 95th-percentile quantified natural variability in seawater properties during the March 2018 survey itself, and was determined from vertical-profiles data unaffected by the discharge.

[22] Thresholds represent limits on wastewater-induced changes to receiving-water properties that significantly exceed natural conditions as specified in the discharge permit and COP. They are determined from the sum of columns to the left and are specific to the March 2018 survey. They do not include the COP allowances specified in the column to the right.

[23] The discharge permit, in accordance with the COP, allows excursions in seawater properties that depart from natural conditions by specified amounts. DO cannot be "*depressed more than 10% from that which occurs naturally*," and pH cannot be "*changed more than 0.2 units from that which occurs naturally.*" The California Thermal Plan is incorporated into the COP by reference, and restricts temperature increases to less than 2.2ºC.

[24] Permit limits P5 and P6 (Table 6) include specific numerical values promulgated in the RWQCB Basin Plan (1994) in addition to changes relative to natural conditions specified in the COP. The Basin Plan upper-bound pH objective for ocean waters is 8.5, but a more-stringent upper-bound objective of 8.3, which applies to individual beneficial uses, was implemented in the MBCSD discharge permit.

[25] Maximum or minimum value measured during the March 2018 survey, regardless of location within or beyond the ZID

As discussed previously, anomalies in multiple seawater properties clearly delineated the plume, but those entrainment-generated excursions were not caused by the presence of wastewater constituents. During periods when the water column is even slightly stratified, ambient seawater properties near the seafloor differ from those within the rest of the water column, and their juxtaposition within the rising effluent plume appears as lateral anomalies within the upper water column. Regardless, if the presence of wastewater particulates had contributed to the observed decreases in DO, pH and transmissivity within the upper water column, their influence would still have been well within the natural range of the ambient seawater properties at the time of the survey. Consequently, their influence on water quality would not be considered environmentally significant.

Other Lines of Evidence

Several additional lines of evidence further support the conclusion that all the CTD measurements collected during the March 2018 survey complied with the quantitative permit limits P3 through P6 in Table 6. In combination, these lines of evidence provide the "best explanation" of the origin and significance of individual measurements using abductive inference (Suter 2007). This process, which has been used to implement sediment-quality guidelines for California estuaries (SWRCB 2009), emphasizes a pattern of reasoning that accounts for both discrepancies and concurrences among multiple lines of evidence. A best explanation approach serves to limit the uncertainty associated with each individual CTD measurement, and to provide a more robust compliance assessment. Together, these lines of evidence significantly strengthen the conclusion that the discharge fully complied with the permit at the time of the March 2018 survey.

Natural Variability within and beyond the ZID: Although the permit limits only apply to changes in DO, pH, temperature, and transmissivity beyond the ZID, examination of measurements acquired within the ZID frequently provides additional insight into the potential for adverse effects on water quality. However, among all the data collected during the March 2018 survey, salinity was the only seawater property that exhibited a perceptible difference from ambient conditions. Regardless of their association with the plume's effluent salinity signature or their proximity to the diffuser structure, none of the 11,033 temperature, DO, pH, and transmissivity observations exceeded their respective thresholds of natural variability specified in Table 8. This is apparent from a comparison between the extrema listed in the last data column in Table 8, and the corresponding natural-variability thresholds listed in third data column. For example, ambient seawater temperatures are expected to range as high as 13.46ºC, but the highest measured temperature was 12.72ºC. Similarly, natural excursions in transmissivity are expected to range as low as 81.5%, while the lowest measured transmissivity was 90.9%.

COP Allowances: The COP does not require that wastewater-induced changes remain within the natural-variability ranges listed in the third data column of Table 8, even though these ranges were conservatively used in the data screening process described in previous subsections. Consideration of COP allowances for some of the receiving-water limits provides an additional safety factor in the compliance evaluation of thermal, DO, and pH excursions.

For pH, the COP and the discharge permit allow changes up to 0.2 pH units from natural conditions, bringing the minimum allowed pH down to 7.746 for the March 2018 survey (fourth data column of Table 8). This limiting value is significantly less than the lowest pH measurement of 8.031 recorded during the March 2018 survey.[26] Similarly, the lowest DO concentration measured during the survey (6.82 mg/L) was well above the lower bound in expected natural variability (5.50 mg/L) and even farther above the much-less-stringent 10% compliance threshold promulgated by the COP (4.95 mg/L).

[26] Compliance with COP maximum pH allowance (8.418) is irrelevant because effluent on the day of the survey had a pH of 7.2, which is much lower than the lowest pH measured within the receiving seawater (8.031). Consequently, the presence of effluent constituents could not have induced an increase in pH within receiving waters.

Insignificant Thermal Impact: As with transmissivity, there are no explicit numerical objectives for discharge-related increases in temperature. Nevertheless, a numerical limit can be established for thermal excursions that is based on the requirement that they not adversely affect beneficial uses (P3 in Table 6). Although the COP remains silent regarding allowable temperature changes, it incorporates the California Thermal Plan requirements by reference (COP Introduction §C.3). The Thermal Plan (SWRCB 1972) restricts temperature increases caused by new discharges to coastal water to be less than 2.2°C (4°F). As with DO and pH, a quantitative permit limit on temperature increases can be established by combining the Thermal Plan allowance with the natural variability threshold listed in the third data column of Table 8. Accordingly, increases in temperature caused by the discharge of warm wastewater during the March 2018 survey could be deemed to adversely affect beneficial uses if they exceeded 15.66°C (fourth data column of Table 8). However, none of the 11,033 CTD measurements collected during the survey exceeded 12.72°C (last column in Table 8). As a result, all the measurements remained well within the natural variability thermal threshold (13.46°C), and provided a much larger safety factor for compliance with the numerical limit derived from the Thermal Plan (15.66°C). In reality, temperatures measured within the rising effluent plume were uniformly below that of the surrounding seawater because cooler seawater near the seafloor had been entrained in the plume shortly after discharge. Consequently, any potential thermal impact resulting from the discharge of warm wastewater was almost immediately eliminated upon discharge because the effluent entrained large volumes of much colder seawater near the seafloor.

Directional Offset: Analysis of the directional offset of CTD measurements is useful because wastewater and receiving-seawater properties depart from one another in several predictable ways. Specifically, upon discharge, wastewater is fresher, warmer, more turbid, and less dense than the ambient receiving waters of Estero Bay. As such, the introduction of wastewater constituents will reduce the salinity, density, and transmissivity of the receiving seawater (negative offset), while temperature will be increased (positive offset). Therefore, the reduced temperatures observed in conjunction with the effluent plume during the tow surveys (Figures 9a and 10a) could not have been generated by the presence of warmer wastewater constituents. Instead, as described above, they were produced because the plume entrained cooler bottom water shortly after discharge, and then transported it upward in the water column where ambient seawater temperatures were higher.

Insignificant Wastewater Particulate Loads: Another independent line of evidence demonstrates that the discharge of wastewater particulates could not have contributed materially to turbidity within the dilute effluent plume, even before completion of the initial mixing process. The effluent suspended-solids concentration measured onshore at the time of the survey was 31 mg/L. After dilution by at least 272 fold, the effluent suspended-solids concentration would have the reduced ambient transmissivity by no more than 0.9%.

Similarly, the MBCSD discharge could not have contributed materially to the observed DO fluctuations. The MBCSD treatment process routinely removes 80% or more of the organic material, as demonstrated by the 32-mg/L BOD measured within the plant's effluent two days after the survey. That small amount of BOD would have induced a DO depression of no more than 0.022 mg/L after dilution (MRS 2002). In fact, in the absence of a tangible BOD influence, wastewater discharge would actually be expected to increase DO within subsurface receiving waters, rather than decrease it. This is because effluent is oxygenated by recent contact with the atmosphere during the treatment process, whereas receiving waters at depth are typically depleted in DO due to the long absence of atmospheric equilibration within the deep offshore watermass.

Excursions remained within the fixed Basin-Plan Limits: Permit provisions P5 and P6 (Table 6) combine receiving-water objectives from both the COP and the Basin Plan with regard to DO and pH

limits. As described previously, the COP requires that DO concentrations outside the ZID not be depressed more than 10% from that which occurs naturally, and restricts pH measurements to those within 0.2 units of that which occurs naturally. In contrast, the Basin-Plan's fixed numerical limits do not provide specific guidance as to how they might change in response to widespread changes in oceanographic conditions unrelated to the discharge. Specifically, the fixed numerical limits restrict DO concentrations outside the ZID to no less than 5 mg/L (P5 in Table 6), and pH levels to the 7.0-to-8.3 range (P6). As such, the fixed Basin-Plan limit on DO is slightly more restrictive than the 4.95 mg/L minimum allowable DO concentration established for the March 2018 survey under COP objectives. Consequently, all of the DO measurements also easily complied with the Basin-Plan limit on DO reductions. The minimum allowable pH (7.0) specified in the Basin Plan was less restrictive than the COP limit (7.746) specified for the March 2018 Survey, so all the pH observations again complied with both regulations.

CONCLUSIONS

The quantitative screening analysis demonstrated that all measurements recorded during the March 2018 survey complied with the receiving-water limitations specified in the NPDES discharge permit. This conclusion was further strengthened by other lines of evidence supporting compliance with the discharge permit. Specifically, although discharge-related changes in seawater properties were observed during the March 2018 survey, the changes were either not of significant magnitude (i.e., they were within the natural range of variability that prevailed at the time of the survey), were measured within the boundary of the ZID where initial mixing is still expected to occur, or were not directly caused by the presence of wastewater constituents within the water column (i.e., were entrainment generated).

Early in the initial mixing process, effluent was being diluted to levels in excess of 272-fold, which is double the critical dilution levels predicted by dispersion modeling after completion of the mixing process. As the negatively buoyant plume descended after first impinging on the sea surface, the initial mixing process was nearly complete and dilution levels exceeded 322-fold. All of the measured dilution levels far exceed levels that were predicted by modeling and that were incorporated in the discharge permit as conservative limits on contaminant concentrations within effluent prior to discharge. Lastly, all of the auxiliary observations collected during the March 2018 survey demonstrated that the discharge complied with the narrative receiving-water limits in the discharge permit and the COP. Together; these observations demonstrate that the treatment process, diffuser structure, and the outfall continue to surpass design expectations.

REFERENCES

Davis, R.E., J.E. Dufour, G.J. Parks, and M.R. Perkins. 1982. Two Inexpensive Current-Following Drifters. Scripps Institution of Oceanography, University of California, San Diego, La Jolla, California. SIO Reference No. 82-28. December 1982.

Fischer, H.B., E.J. List, R.C.Y. Koh, J. Imberger, and N.H. Brooks. 1979. Mixing in Inland and Coastal Waters. New York: Academic Press, 482 p.

Kuehl, S.A., C.A. Nittrouer, M.A. Allison, L. Ercilio, C. Faria, D.A. Dukat, J.M. Jaeger, T.D. Pacioni, A.G. Figueiredo, and E.C. Underkoffler 1996. Sediment deposition, accumulation, and seabed dynamics in an energetic fine-grained coastal environment. *Continental Shelf Research*, 16: 787-816.

Marine Research Specialists (MRS). 1998. City of Morro Bay and Cayucos Sanitary District, Offshore Monitoring and Reporting Program, Semiannual Benthic Sampling Report, April 1998 Survey. Prepared for the City of Morro Bay, CA. July 1998.

Marine Research Specialists (MRS). 2002. City of Morro Bay and Cayucos Sanitary District, Supplement to the 2002 Renewal Application For Ocean Discharge Under NPDES Permit No. Prepared for the City of Morro Bay and Cayucos Sanitary District, Morro Bay, CA. July 2002.

Marine Research Specialists (MRS). 2011. City of Morro Bay and Cayucos Sanitary District, Offshore Monitoring and Reporting Program, 2010 Annual Report. Prepared for the City of Morro Bay, California. March 2011.

Marine Research Specialists (MRS). 2012. City of Morro Bay and Cayucos Sanitary District, Offshore Monitoring and Reporting Program, 2011 Annual Report. Prepared for the City of Morro Bay, California. March 2012.

Marine Research Specialists (MRS). 2013. City of Morro Bay and Cayucos Sanitary District, Offshore Monitoring and Reporting Program, 2012 Annual Report. Prepared for the City of Morro Bay, California. March 2013.

Marine Research Specialists (MRS). 2014. City of Morro Bay and Cayucos Sanitary District, Offshore Monitoring and Reporting Program, 2013 Annual Report. Prepared for the City of Morro Bay, California. March 2014.

National Academy of Sciences. 1993. Managing Wastewater in Coastal Urban Areas. National Research Council Committee on Wastewater Management for Coastal Urban Areas, Water Science and Technology Board, Commission on Engineering and Technical Systems. 477 pp.

Regional Water Quality Control Board (RWQCB) - Central Coast Region. 1994. Water Quality Control Plan (Basin Plan) Central Coast Region. Available from the RWQCB at 81 Higuera Street, Suite 200, San Luis Obispo, California. 148p. + Appendices.

Regional Water Quality Control Board (RWQCB) - Central Coast Region and the Environmental Protection Agency (USEPA) – Region IX. 1992a. Waste Discharge Requirements (Order No. 92-67) and Authorization to Discharge under the National Pollutant Discharge Elimination System (Permit No. CA0047881) for City of Morro Bay and Cayucos Sanitary District, San Luis Obispo County.

Regional Water Quality Control Board (RWQCB) - Central Coast Region and the Environmental Protection Agency (USEPA) – Region IX. 1992b. Monitoring and Reporting Program No. 92-67 for City of Morro Bay and Cayucos Sanitary District, San Luis Obispo County (Permit No. CA0047881).

Regional Water Quality Control Board (RWQCB) - Central Coast Region and the Environmental Protection Agency (USEPA) – Region IX. 1998a. Waste Discharge Requirements (Order No. 98-15) and National Pollutant Discharge Elimination System (Permit No. CA0047881) for City of Morro Bay and Cayucos Sanitary District, San Luis Obispo County. 11 December 1998.

Regional Water Quality Control Board (RWQCB) - Central Coast Region and the Environmental Protection Agency (USEPA) – Region IX. 1998b. Monitoring and Reporting Program No. 98-15 for City of Morro Bay and Cayucos Sanitary District, San Luis Obispo County. 11 December 1998.

Regional Water Quality Control Board (RWQCB) - Central Coast Region and the Environmental Protection Agency (EPA) – Region IX. 2009. Waste Discharge Requirements (Order No. R2-2008-0065) and National Pollutant Discharge Elimination System (Permit No. CA0047881) for the Morro Bay and Cayucos Wastewater Treatment Plant Discharges to the Pacific Ocean, Morro Bay, San Luis Obispo County. Effective 1 March 2009.

Sea-Bird Electronics, Inc. (SBE) 1989. Calculation of M and B Coefficients for the Sea-Tech Transmissometer. Application Note No. 7, Revised September 1989.

Sea-Bird Electronics, Inc. (SBE) 1992. SBE 12/22/22/20 Dissolved Oxygen Sensor Calibration and Deployment. Application Note No. 12-1, rev B, Revised April 1992.

Southern California Bight Field Methods Committee (SCBFMC). 2002. Field Operation Manual for Marine Water-Column, Benthic, and Trawl monitoring in Southern California. Technical Report 259. Southern California Coastal Water Research Project. Westminster, CA. March 2002.

State Water Resources Control Board (SWRCB). 1972. Water Quality Control Plan for Control of Temperature in the Coastal and Interstate Waters and Enclosed Bays and Estuaries of California. Revises and supersedes the policy adopted by the State Board on January 7, 1971, and revised October 13, 1971, and June 5, 1972. California Division of Water Quality, Water Quality Planning Unit.

State Water Resources Control Board (SWRCB). 2005. Water Quality Control Plan, Ocean Waters of California, California Ocean Plan. California Environmental Protection Agency. Effective February 14, 2006.

State Water Resources Control Board (SWRCB). 2009. Water Quality Control Plan for Enclosed Bays and Estuaries – Part 1 Sediment Quality. California Environmental Protection Agency. Effective August 22, 2009. sed_qlty_part1.pdf [Accessed 02/26/10].

Suter II, Glenn, W. 2007. Ecological risk assessment, 2nd edition. U. S. Environmental Protection Agency, Cincinnati, Ohio. CRC.

Tetra Tech. 1992. Technical Review City of Morro Bay, CA Section 201(h) Application for Modification of Secondary Treatment Requirements for a Discharge into Marine Waters. Prepared for the U.S. Environmental Protection Agency, Region IX, San Francisco, CA by Tetra Tech, Inc., Lafayette, CA. February 1992.